Simulation and factor analysis for post-earthquake recovery of densely populated urban residential communities in China

Qian Tao[a], Zheng He[a,b]*, Haijiang Li[c]

[a]*Department of Civil Engineering, Dalian University of Technology, Dalian, China*;

[b]*State Key Laboratory of Coastal and Offshore Engineering, Dalian University of Technology, Dalian, China*;

[c]*Cardiff School of Engineering, Cardiff University, Cardiff, U.K.*

*E-mail: hezheng@dlut.edu.cn; Tel & Fax: +86-411-84707500

Factor sensitivity and correlation analysis for the post-earthquake recovery simulation of densely populated urban residential communities in China

Abstract: Earthquake disasters in recent decades have caused huge socioeconomic losses in China, while post earthquake recovery simulation is crucial for resilient community planning, different interconnected aspects and numerous factors are required to be considered and analyzed holistically, and that makes the process is highly complex especially cascading with the long time recovery duration. To identify the key infrastructural characteristics that affect the post-earthquake recovery of densely populated urban residential communities (URCs) in China, a comprehensive framework of resilience assessment and analysis is established on a systematic integration of multiple analysis tools (e.g., population-based functionality indicators, post-earthquake recovery simulations, infrastructural dependence analyses, and seismic damage analyses). The framework can consider the dependence among residential buildings, supporting buildings, and utility networks, as well as the relationships between their functionalities and resident outmigration; it also includes infrastructural repair sequences at different levels to allow flexible repair plans to be simulated. A case study was used to conduct factor sensitivity and correlation analysis to clarify the effects of three important infrastructural characteristics. Results show that improvements on the seismic performance of residential buildings facilitate community recovery more significantly than utility networks, and the use of redundant utility pipelines can hardly impact the recovery of URCs. However in long term recovery cases, utility networks play more important role due to the cascading effects arising from the extension of the repair durations. The proposed methodology and framework can promote significantly the understanding of community recovery, and the results demonstrate the effectiveness of identifying key influential factors. Such a framework can be further expanded for post earthquake recovery holistic decision making.

Keywords: Earthquakes; Infrastructure; Buildings, residential; Resilience; Simulation.

Introduction

Severe earthquake disasters in recent decades have caused huge socioeconomic losses in China. Nowadays, some megacities in China are still attacked by earthquakes occasionally. Researching and promoting the strategy of community resilience is critical to reducing the risk of seismic loss of these cities and their densely populated communities. Many models, methodologies, and computational tools have been proposed to perform the design and assessment of the resilience of urban residential communities (URCs) (Shadabfar et al. 2022). Related studies (Miles et al. 2019; Koliou et al. 2020) typically assess seismic resilience in three steps: indicating the performance of a targeted system, drawing a curve of the performance recovery, and quantifying resilience with a value mapped from the curve. The definition of performance indicators, the description of repair sequences, and the selection of resilience metrics are critical to these three steps.

In resilience assessments, the selection of performance indicators should be considered carefully, since their inappropriate usage can yield incorrect assessment result (Poulin and Kane 2021). Some representative indicators have been established: patient waiting time (Cimellaro et al. 2010), average number of pathways (Zhang et al. 2017), etc. Because these indicators are highly correlated to their targeted systems, they are difficult to apply to complex systems, such as a URC with multiple infrastructures. Some studies described the functional dependence between different infrastructures, e.g., the dependence between an electricity power network and a water network (Dueñas-Osorio et al. 2007). However, the gas and telecom networks which are common in URCs of China were not considered, which may affect the functional quantification of buildings. Furthermore, the damages of these lifelines may lead to secondary disasters, which need more attention and better understanding (Freddi et al. 2021).

Because the human factors (e.g., risk awareness and scenario training) receives growing attention in the field of infrastructure resilience currently (Cantelmi et al. 2021), some studies (Burton et al. 2016; Feng et al. 2017) preferred to indicate community performance using non-engineering factors (e.g., population). However, these studies did not distinct the effects of functional losses of different buildings and the caused different kinds of resident outmigration. Burton et al. (2019) used an empirical utility-based decision model to analyze the impacts of residence time, physical damage, household income, and several other factors on household decision-making, but they did not consider the potential effects of different stakeholders. Some studies (Nejat and Ghosh 2016; Masoomi et al. 2018) attempted to analyze multiple factors influencing household decision-making and post-disaster outmigration. However, their focus was on meteorological hazards rather than earthquakes. Methods that can synthetically characterize the resilience of social and technical systems are a promising research stream (Cantelmi et al. 2021). One important relevant area is inviting stakeholders in the resilience assessment (Poulin and Kane 2021). Some resilience assessments integrated with multiple stakeholder-related factors were proposed by sociology-based studies (Cai et al. 2018), but their description of physical infrastructures is relatively insufficient.

With respect to describing repair sequences, the impacts of this factor have been studied for water-supply networks (Chang et al. 2002), power-supply networks (Ouyang and Dueñas-Osorio 2014), etc. FEMA P-58 (FEMA 2012) and REDi (Almufti and Willford 2013) integrated some practical factors related to repair sequences of buildings into their analysis methodology. However, these studies just focus on different types of utility networks or single buildings. The study of repair sequences specifically for a URC is still lacking. Based on the recovery curves calculated from the repair sequences, retrofitting techniques can be introduced effectively according to the resilience assessment results (Yin et al. 2022). Besides, resilience assessment frameworks should have the ability to mathematically unify downtime predictions for both physical and non-physical factors, so that the post-earthquake recovery can be quantified more accurately (Freddi et al. 2021).

In order to improve the effectiveness of resilience assessments, the resilience of a community is considered and measured in multidisciplinary and multicriteria methodologies (Yin et al. 2022). Existing studies have proposed various metrics with different characteristics, such as the classical seismic resilience metric (Bruneau et al. 2003), the metric reflecting the performance before and after earthquakes (Cimellaro et al. 2010), and the threshold metric established on dynamics (Tao and He 2020a). Because these metrics are only values compressed from the information carried by recovery curves, the assessment results obtained from such single values may be too one-sided.

More importantly, the key factors of the recovery of a URC are still unclarified. The coexistence of different kinds of factors (e.g., network topology, seismic fragility of buildings) and their interactions haven't gotten enough attention, although they are very common in real URCs. This issue brings great challenges to the subsequent resilience-oriented design and optimization in term of selecting design variables and making calculation plans (Shadabfar et al. 2022). Currently, there is still a lack of a resilience assessment methodology that can integrate these factors from the perspective of URCs, as well as a comprehensive understanding of their impacts by a unified standard.

In order to facilitate a more in-depth understanding of community recovery and provide a theoretical basis for resilience-based design and optimization, this paper aims to propose an innovative methodology for resilience assessment and analysis that is expected to clarify the key factors of the recovery of URCs. The methodology is built on the systematical integration of several specialized analysis tools constructed in this paper (i.e., the infrastructural dependence model, the population-based functionality indicator, and the repair sequence function) and some existing well-established models (e.g., seismic damage models, resilience metrics). On this basis, a case study is conducted with a typical Chinese densely populated URC. Since the assessment needs performing dozens of times in the analysis, a small-scale URC is chosen as the case to reduce the analysis costs. Although its scale is limited, this URC has a complete infrastructural system which can fully satisfy the requirement of the analysis. With these efforts, it is found that the recovery of a URC can be promoted more significantly by improving the seismic performance of residential buildings than by improving it of other infrastructures. The impacts of network redundancy and internetwork cascading are unobvious, but they need more attention if the repairs of utility networks are time-consuming.

Conceptual model of URCs

Community function and structure

To meet the daily needs of residents, various sectors that provide different services (e.g., housing, police, and retail) operate in URCs. In this study, four sectors, whose continuous functioning is very helpful to stabilize a community (Cutter et al. 2010) are considered: housing, education, commercial retail, and medical care. To support these services, buildings and utility networks are built in URCs. In order to distinct different kinds of outmigration hereinafter, buildings are divided into residential buildings and supporting buildings. Specifically, supporting buildings are a general term for educational buildings, commercial buildings, and medical buildings. Four typical utility networks that are essential for URCs are considered: the networks of electricity, telecommunication, tap water, and natural gas. The telecom network particularly refers to a wired network composed of optical cables. Transportation networks are not considered since their high complexity can significantly increase the difficulty of the following recovery simulation and resilience analysis. This simplification may make the analysis results more optimistic than the actual situations, because the seismic damage of a transportation system can hinder the repairs of buildings and utility networks. However, the difference decreases as the scale of the transportation system reduces. Because the scale of transportation networks of Chinese densely populated URCs which usually consist of several high-rise buildings is commonly small, this simplification is acceptable for such communities. As the users of a URC, residents are another indispensable part. Fig. 1 summarizes the relationships between residents and infrastructures, as well as the infrastructural composition defined in this study.

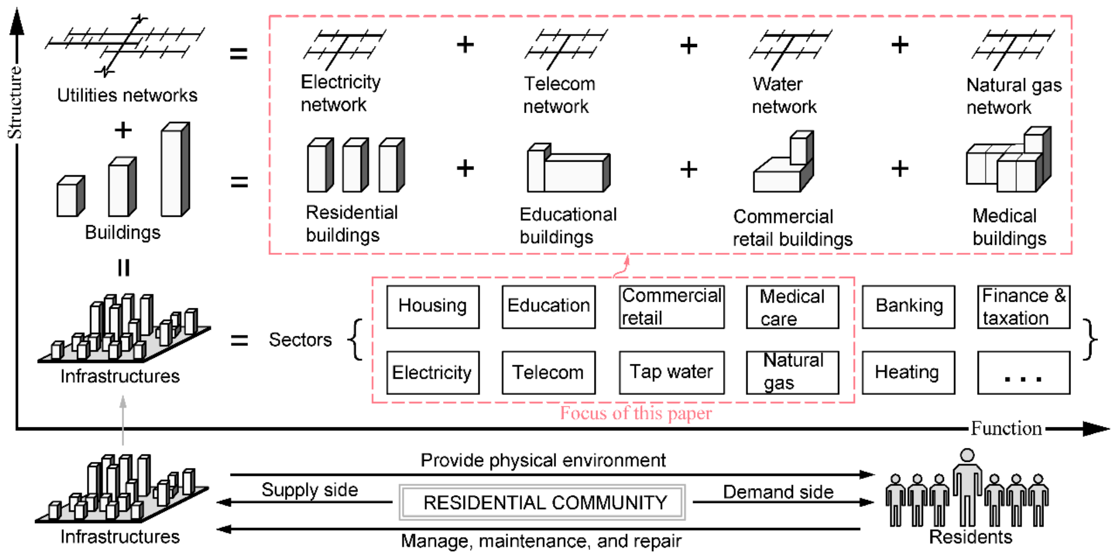

Fig. 1. Conceptual illustration of URC model

Sectors and infrastructures

In a densely populated URC, the number of residential buildings is typically much more than the number of supporting buildings. Therefore, the housing sector is described in detail by multiple buildings, while the other three sectors are each represented by a single building. This simplification is only applicable to small-scale

URCs whose supporting facilities are relatively few. For large-scale URCs, it is still recommended to employ multiple buildings to describe the related sectors. To reduce calculation costs, the seismic damages and recoveries of buildings are depicted at the building level.

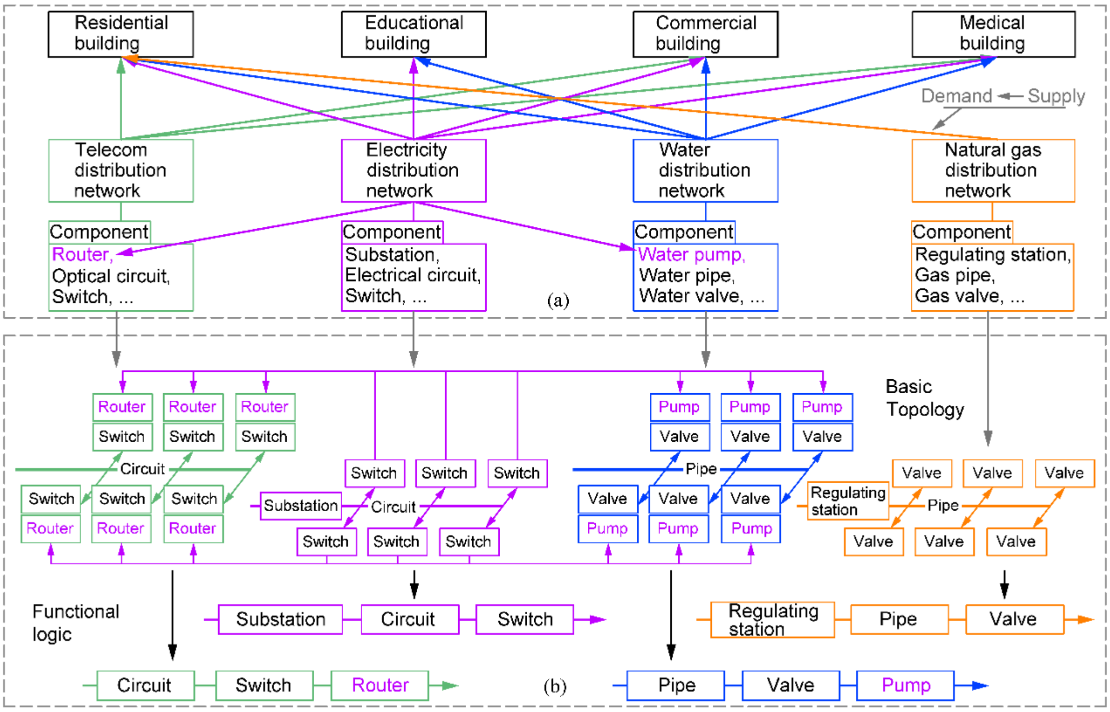

Fig. 2. Infrastructural components and their functional dependence; (a) Utility dependence; (b) Topology and functional logic of utility networks

The utilities on which each building depends are described in Fig. 2(a). Dependence also exists between utility networks. For example, electricity is required by telecommunication routers and water pumps [see Fig. 2(b)]. For densely populated URCs where high-rise residential buildings are intensively built, routers and pumps are typically installed in a dispersed manner in the equipment rooms of each building. Utility networks are commonly described by topology models or flow models.

Topology models can reflect the adjacent relationship of the components of a network (Boccaletti et al. 2006). Based on the adjacent relationship, the failure risk of utility networks can be assessed using damage probabilities of their components. Flow models further consider the motion states of material flows. Thus, both their accuracy and computational costs are higher than those of topology models. Because the community performance is primarily associated with the functionalities of buildings in this study, topology models are basically sufficient to meet the analysis needs. The fragility data of utility networks needed in analysis can be found in relevant references (Isoyama et al. 2000; Loganathan et al. 2002; FEMA 2013).

Resident population and outmigration

The population served by a URC can be regarded as a performance indicator. After earthquakes, infrastructural damages which always bring inconvenience to residents will degrade the dependent attitudes of residents on their communities, ultimately resulting in outmigration. Due to the complex demographic structure of densely populated URCs, the reasons for post-earthquake outmigration are diverse. Unlike existing studies that consider outmigration as a whole, herein, the outmigration is divided into two categories in accordance with the functional types of the related buildings. This change is conducive to a clearer quantification of resident population. Primary outmigration (POM) is caused by the dysfunction of residential buildings. Because the residents have to move out when a residential building becomes unsafe, POM is typically mandatory. POM can be quantified by the loss of occupiability (Burton et al. 2016; Tao and He 2020b). Secondary outmigration (SOM) is caused by the dysfunction of supporting buildings. SOM has a smaller impact on residents than POM, because supporting buildings are functionally replaceable due to their public nature.

Because SOM depends significantly on the dependent attitudes of residents on the community, two sociological methodologies [i.e., the residential satisfaction model (Gifford 2007) and disability weightings (Murray 1994)] which receive little attention in resilience-related studies are employed herein to quantify SOM. The residential satisfaction model quantifies the importance of supporting buildings to the dependent attitudes of residents (Gifford 2007). The weights of its membership function can be used to calculate the SOM caused by a single supporting building. Disability weightings (Murray 1994) are a tool used in calculating the effects of different types of disabilities. If the impacts of dysfunction of supporting buildings on residents are equivalent to the restrictions of disabilities on human life, the ratio of disability weightings can be used to estimate the couplings in the SOM caused by multiple supporting buildings.

Post-earthquake recovery simulation of community

Probabilistic seismic performance model

Based on the conceptual model, the infrastructures are abstracted into entities of three levels: facility groups (FGs), sectors (STs), and basic components (BCs). The seismic performance model can be established on these entities (see Fig. 3). The rugged components (i.e., valves and switches) and specialized equipment systems (i.e., substation and regulating station) shown in Fig. 2 are not considered.

For a utility network, because its source node (SR) and sink node (SN) will be connected if any of their pathways are passable, their connection probability can be calculated by:

$$P_{SR\&SN,C}\left(t\right)=1-P_{SR\&SN,DC}\left(t\right)=1-\prod_{d=1}^{N_{PW}}P_{PW_d,IP}\left(t\right) \quad (1)$$

where N_{PW} is the number of pathways; $P_{SR\&SN,C}(t)$ and $P_{SR\&SN,DC}(t)$ are the connection and disconnection probability respectively; $P_{PWd,IP}(t)$ is the probability that the d^{th} pathway is impassable; and t is the time variable. Specifically, the recovery efforts start at the time t=0. Because the components of a pathway are connected in series, the passable probability [i.e., $P_{PW,P}(t)$] is equal to the product of the functioning probabilities of all related components. Thus, $P_{PW,IP}(t)$ and $P_{PW,P}(t)$ can be calculated by:

$$P_{PW,IP}\left(t\right)=1-P_{PW,P}\left(t\right)=1-\prod_{e=1}^{N_{UC}}P_{UC_e,F}\left(t\right) \quad (2)$$

where, N_{UC} is the number of UCs (i.e., utility components) on the pathway; the subscript, UC_e, represents the e^{th} utility component; and $P_{UCe,F}(t)$ is the probability that UC_e is functioning well.

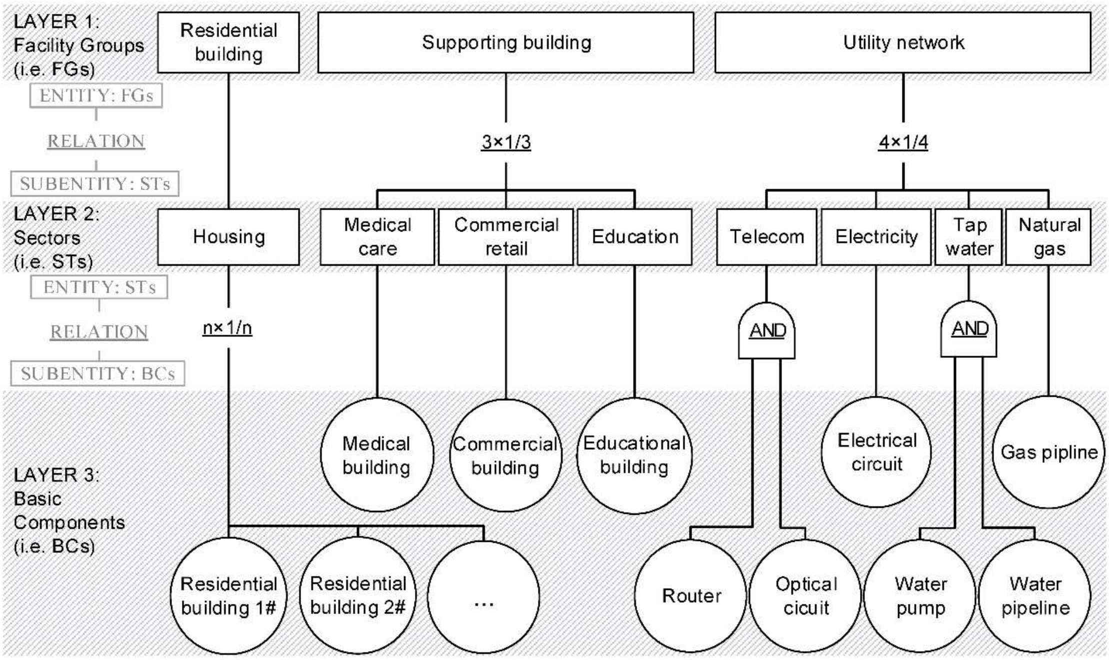

Fig. 3. Infrastructural hierarchy and concerned entities

Pipelines and cables that are utility-independent (UID) can function effectively as long as they are operable. Pumps and routers which are utility-dependent (UD) cannot operate without electricity. Thus, the functioning probability of these two types of components can be calculated by:

$$P_{UC,F}\left(t\right)=\begin{cases}P_{UC,O}\left(t\right) & UC\in UID\\ P_{UC,O}\left(t\right)\prod_{a'=1}^{N_{UN(UC)}}\left[1-\alpha_{UC/SR_{a'}}P_{SR_{a'}\&UC,DC}\left(t\right)\right] & UC\in UD\end{cases} \tag{3}$$

where, $N_{UN(UC)}$ is the number of utility networks on which the UC depends; the subscript, $SR_{a'}$, represents the source node of the a'^{th} utility network on which the UC depends; and $P_{SR_{a'}\&UC,DC}(t)$, the probability that the UC and $SR_{a'}$ are disconnected, can be calculated using Eqn. (1). In a single-source network, $P_{SR_{a'}\&UC,DC}(t)$ is equivalent to the probability that the UC loses the supply of the utility. Unlike other existing probabilistic performance models of interdependent networks, an additional coefficient $\alpha_{UC/SR_{a'}}$, whose value is between 0 and 1, is used in this study to describe the strength of the dependence of the UC on $SR_{a'}$. The larger $\alpha_{UC/SRa'}$ is, the stronger the dependence is. The probability that the UC is operable [i.e., $P_{UC,O}(t)$], is determined by the probability distribution of damage states of the UC and the corresponding parameters of repair. Its calculation will be given in Eqn. (5). Because this study primarily focuses on resilience assessments, the seismic performance model proposed herein only describes the connectivity of networks without considering their supply qualities. If more accurate analysis results are required, other specialized analysis methods for utility networks need incorporating further.

Because the normal functioning of a building requires an occupiable structure and available utilities [see Fig. 2(a)], the probability that a building (BD) is functional or dysfunctional [i.e., $P_{BD,F}(t)$ or $P_{BD,DF}(t)$] can be calculated by:

$$P_{BD,F}\left(t\right)=P_{BD,O}\left(t\right)\prod_{a'=1}^{N_{UN(BD)}}P_{SR_{a'}\&BD,C}\left(t\right) \tag{4a}$$

$$P_{BD,DF}\left(t\right)=1-P_{BD,F}\left(t\right) \tag{4b}$$

where, $N_{UN(BD)}$ is the number of utility networks on which the building depends; $P_{SRa'\&BD,C}(t)$, the probability that the building and $SR_{a'}$ are connected, is calculated by Eqn. (1). In a single-source network, $P_{SRa'\&BD,C}(t)$ is equivalent to the probability that the building can obtain the a^{th} utility. $P_{BD,O}(t)$ is the probability that the building is occupiable. Its calculation method is similar to $P_{UC,O}(t)$ [see Eqn. (5)]. According to Eqn. (4), three functional states of buildings are defined: unoccupiable, occupiable, and fully functional. The first two states are collectively called the dysfunctional state herein. The definitions of these states can be found in existing research (Burton et al. 2016).

If utility components and buildings are collectively identified as BCs, $P_{UC,O}(t)$ in Eqn. (3) and $P_{BD,O}(t)$ in Eqn. (4) can be rewritten as $P_{BC,O}(t)$ together. BC represents the basic component. If a BC is respectively in the inoperable (or unoccupiable) state and operable (or occupiable) state before and after the repair, $P_{BC,O}(t)$ can be calculated by the sum of probabilities of the damage states whose repairs haven been finished before time t (Burton et al. 2016; Miles et al. 2019) [see Fig. 4(b)]:

$$P_{BC,O}\left(t\right) = \sum\nolimits_{n=1}^{N_{DS(BC)}} \mathrm{H}_{BC,DS_n}\left(t\right) P_{BC,DS_n} \tag{5}$$

where, $N_{DS(BC)}$ is the number of damage states; the subscript, DS_n, represents the n^{th} damage state; and $H_{BC,DSn}(t)$ is the step function that depicts the operability jump occurred when the BC is repaired. More details about $H_{BC,DSn}(t)$ will be specifically introduced in the next section. $P_{BC,DSn}$, the probability that the BC is in DS_n, is estimated using fragility functions [see Fig. 4(a)].

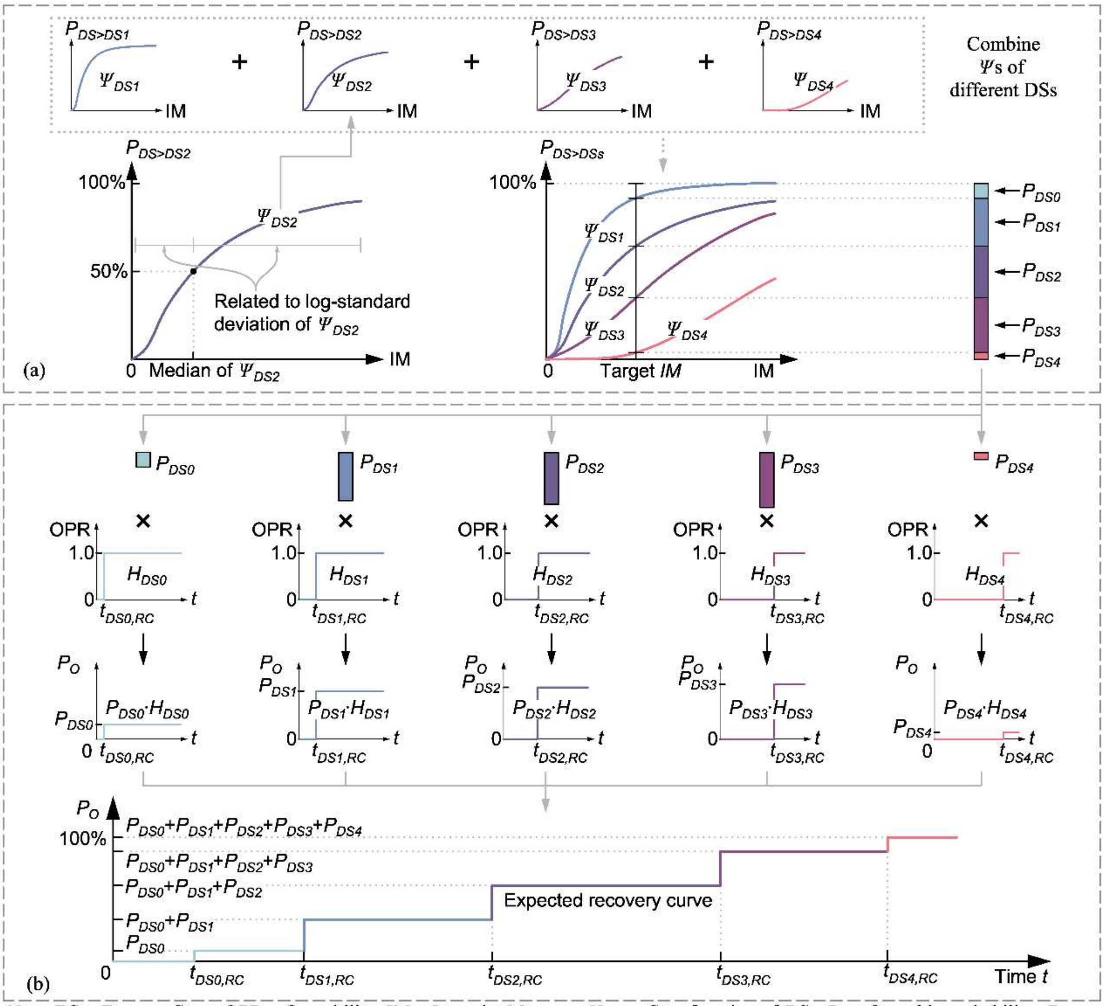

Note: DS = Damage State; OPR = Operability; IM = Intensity Measure; H_{DSn} = Step function of DS_n; P_O = Operable probability; P_{DSn} = Probability of DS_n; $P_{DS>DSn}$ = Exceedance probability of DS_n; $t_{DSn,RC}$ = Repair completion time of DS_n; Ψ_{DSn} = Lognormal cumulative distribution function of DS_n.

Fig. 4. Method to depict expected recovery path of BCs; (a) Calculation of probabilities of damage states; (b) Drawing of expected recovery path

Fragility curves are commonly depicted by the lognormal cumulative distribution function (CDF) [i.e., $\Psi(\cdot)$]. Although this function may be inadequate to model the failure probability of some vulnerable components, it can still accurately describe the seismic fragility of most infrastructures. Some widely-used technical manuals and guides (FEMA 2012; FEMA 2013; Pitilakis et al. 2014) still consider it as the primary method to describe infrastructural seismic fragilities. Correspondingly, the probability that a BC is in a certain DS (i.e., $P_{BC,DS}$) can be calculated by $\Psi(\cdot)$:

$$P_{BC,DS} = P_{BC}\left[DS \middle| IM_T\right] = \Psi\left[\ln\left(IM_T / \mu_{BC,DS}\right) / \beta_{BC,DS}\right] \tag{6}$$

where, IM_T is the targeted intensity of ground motions; $\mu_{BC,DS}$ and $\beta_{BC,DS}$ respectively represent the median and log-standard deviation of the intensity of ground motions. They can be assigned with the data provided in existing references (FEMA 2013).

Functions of infrastructural repair sequences

If Eqn. (5) is calculated in each time step, the trend of $P_{BC,O}(t)$ will be shown as a time-varying curve which is called the functional recovery path. This path can be characterized with step functions (Burton et al. 2016; Tao and He 2020b), since the operability of a basic component generally jumps from 0 to 100% when its repair ends:

$$\mathrm{H}_{BC,DS}(t) = \mathrm{H}\left(t - t_{BC,DS,RC}\right) = \begin{cases} 0 & t < t_{BC,DS,RC} \\ 1 & t \geq t_{BC,DS,RC} \end{cases} \tag{7}$$

where, $t_{BC,DS,RC}$ is the repair completion (RC) time of a BC in a certain . It consists of two parts:

$$t_{BC,DS,RC} = t_{BC,RS} + t_{BC,DS,RD} \tag{8}$$

where, $t_{BC,DS,RD}$ is the repair duration (RD) of the BC in the DS. It can be assigned with the data provided in existing references (FEMA 2013; MOHURD 2016). $t_{BC,RS}$, the repair start (RS) time of the BC, is a reflection of the infrastructural repair sequences.

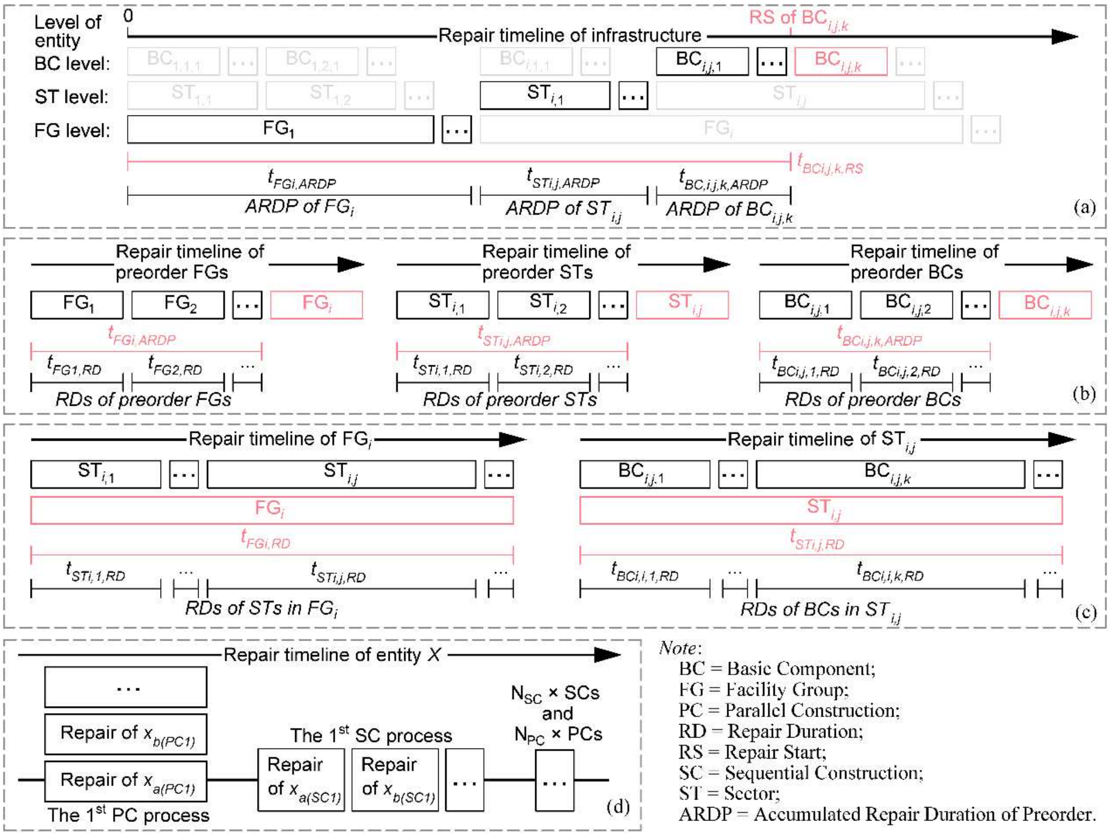

Fig. 5. Temporal structure of infrastructural repair process and calculation method of its parameters; (a) Repair start time of $BC_{i,j,k}$; (b) Accumulative repair durations of preorder entities; (c) Repair duration of FG_i and $ST_{i,j}$; (d) Illustration of repair sequence of arbitrary entity X

In order to calculate $t_{BC,RS}$, it is necessary to clarify the position of the BC in the whole infrastructural system. Herein, the k^{th} basic component of the j^{th} sector ($ST_{i,j}$) in the i^{th} facility group (FG_i) is noted as $BC_{i,j,k}$. With regard to $BC_{i,j,k}$, the FGs repaired before FG_i, the STs repaired before $ST_{i,j}$, and the BCs repaired before $BC_{i,j,k}$ are called the preorder FGs, the preorder STs, and the preorder BCs respectively. According to the calculation method shown in Fig. 5(a), $t_{BCi,j,k,RS}$ is equal to the sum of the accumulative repair durations of these preorder entities (i.e., ARDPs):

$$t_{BC_{i,j,k},RS} = t_{FG_i,ARDP} + t_{ST_{i,j},ARDP} + t_{BC_{i,j,k},ARDP} \tag{9}$$

where, $t_{FGi,ARDP}$, $t_{STi,j,ARDP}$, and $t_{BCi,j,k,ARDP}$ represent the ARDPs of $BC_{i,j,k}$ at the FG level, ST level, and BC level respectively. Since these ARDPs are determined by the repair durations of the corresponding entities [see Fig. 5(b)], ARDPs can be expressed as functions of them:

$$t_{FG_i,ARDP} = G_{RS,FG}\left(\left\{t_{FG_p,RD} \,|\, p \in N_+, 1 \le p \le i-1\right\}\right) = G_{RS,FG}\left(t_{FG_1,RD}, t_{FG_2,RD}, \ \cdots, t_{FG_{i-1},RD}\right) \tag{10a}$$

$$t_{ST_{i,j},ARDP} = G_{RS,ST}\left(\left\{t_{ST_{i,q},RD} \,|\, q \in N_+, 1 \le q \le j-1\right\}\right) = G_{RS,ST}\left(t_{ST_{i,1},RD}, t_{ST_{i,2},RD}, \ \cdots, t_{ST_{i,j-1},RD}\right) \tag{10b}$$

$$t_{BC_{i,j,k},ARDP} = G_{RS,BC}\left(\left\{t_{BC_{i,j,r},RD} \,|\, r \in N_+, 1 \le r \le k-1\right\}\right) = G_{RS,BC}\left(t_{BC_{i,j,1},RD}, t_{BC_{i,j,2},RD}, \ \cdots, t_{BC_{i,j,k-1},RD}\right) \tag{10c}$$

where, the subscripts, p, q, and r, describe the IDs of preorder entities at different levels; $G_{RS,FG}(t)$, $G_{RS,ST}(t)$, and $G_{RS,BC}(t)$ are the functions of repair sequences describing the repair processes of FGs, STs, and BCs respectively. The expression of these functions is introduced in detail in Eqn. (13). $t_{FGp,RD}$, $t_{STi,q,RD}$, and $t_{BCi,j,r,RD}$ represent the repair durations of FG_p, $ST_{i,q}$ and $BC_{i,j,r}$.

Because $t_{FGp,RD}$ and $t_{STi,q,RD}$ are determined by the repair durations of their sub-entities [see Fig. 5(c)], they can be described using $G_{RS,ST}(t)$ and $G_{RS,BC}(t)$ respectively:

$$t_{FG_i,RD} = G_{RS,ST}\left(\left\{t_{ST_{i,q},RD} \,|\, q \in N_+, 1 \le q \le N_{ST}\right\}\right) = G_{RS,ST}\left(t_{ST_{i,1},RD}, t_{ST_{i,2},RD}, \ \cdots, t_{ST_{i,N_{SF}},RD}\right) \tag{11a}$$

$$t_{ST_{i,j},RD} = G_{RS,BC}\left(\left\{t_{BC_{i,j,r},RD} \,|\, r \in N_+, 1 \le r \le N_{BC}\right\}\right) = G_{RS,BC}\left(t_{BC_{i,j,1},RD}, t_{BC_{i,j,2},RD}, \ \cdots, t_{BC_{i,j,N_{BC}},RD}\right) \tag{11b}$$

where, N_{ST} and N_{BC} represent the number of STs in FG_i and the number of BCs in $ST_{i,j}$ respectively. According to Eqn. (11), $t_{BCi,j,r,RD}$ is the basis for calculating $t_{FGi,RD}$ and $t_{STi,j,RD}$. Because the repair duration of a BC is related to the probability distribution of its damage states, $t_{BC,RD}$ can be estimated by the expected repair duration of a BC in its different damage states:

$$t_{BC,RD} = \sum\nolimits_{n=1}^{N_{DS(BC)}} P_{BC,DS_n} t_{BC,DS_n,RD} \tag{12}$$

where, $N_{DS(BC)}$ is the number of damage states; $P_{BC,DSn}$ is the probability that the BC is in the n^{th} damage state (DS_n); and $t_{BC,DSn,RD}$ is the repair duration of the BC. These variables have been introduced in Eqns. (5)~(8). Herein, $t_{BC,DSn,RD}$ and its related time parameters are regarded as deterministic variables in order to simplify the description of the temporal randomness caused by the variability of real repair process. This randomness is difficult to be clarified without exclusively-collected related statistical data. Nevertheless, if related data are sufficient, it is still recommended to assess the impact of variability of repair process using a sensitivity analysis.

Because the repair of an entity can be regarded as a combination of multiple parallel construction processes (PCs) and sequential construction processes (SCs) of its sub-entities [see Fig. 5(d)], the repair sequences of different levels [see Eqns. (10)~(11)] can be described collectively:

$$G_{RS,X}\left(t_{X_1}, t_{X_2}, \dots, t_{X_n}\right) = \sum\nolimits_{i=1}^{N_{SC}} \sum \left[\left\{ t_{X_{p(i)}} \middle| X_{p(i)} \in SC_i \right\}\right] + \sum\nolimits_{j=1}^{N_{PC}} \max\left[\left\{ t_{X_{q(j)}} \middle| X_{q(j)} \in PC_j \right\}\right] \tag{13}$$

where, $G_{RS,X}(t)$ is the function of the repair sequence of the X-level entities. Its independent variables, t_{X1}, t_{X2}, and t_{Xn}, represent the repair durations of the corresponding entities. SC_i represents the i^{th} collection of entities that are repaired sequentially. $X_{p(i)}$ is the p^{th} entity in SC_i. PC_j represents the j^{th} collection of entities that are repaired in parallel. $X_{q(j)}$ is the q^{th} entity in PC_j. N_{SC} and N_{PC} represent the numbers of these two kinds of collections. $t_{Xp(i)}$ and $t_{Xq(j)}$ are the repair durations of $X_{p(i)}$ and $X_{q(j)}$ respectively. In Eqn. (13), the RDs of sequentially repaired entities are joined using summation, while the RDs of simultaneously repaired entities are joined using maximum. Because the repair process is a combination of SCs and PCs, the total RD is calculated by the sum of these summations and maxima. It should be noted that flow repetitive construction operation is not considered in the proposed repair sequence function, which may make the simulation results deviate from actual recovery situations.

Infrastructural characteristics

In this section, three concerned infrastructural characteristics are introduced. First, the seismic fragility reflects the possibility that an infrastructural entity is in a certain damage state when it suffers earthquakes of a certain intensity. Its changes are reflected in the probabilities of damage states of basic components [see Eqn. (6)]. Based on the infrastructural dependence [see Eqns. (1)~(5)], the influences of the changes gradually spread to different sectors, resulting in affecting the entire community. In factor analysis, this influence can be modeled by changing the median (i.e., $\mu_{BC,DS}$) of fragility functions.

Topology describes the adjacent relationships between buildings and pipelines. In densely populated URCs, utility networks are typically designed as simple acyclic dendritic topologies to minimize engineering costs. In some upscale communities with higher seismic design levels, a few of redundant pipelines may be installed to improve the reliability of utility networks. These redundant pipelines may affect the probabilities that buildings obtain utilities, resulting in changing their functional states. In factor analysis, the impact of topological redundancy (i.e., γ_{UN}) is characterized by the numbers of pathways between the source nodes and sink nodes [see Eqn. (1)].

Internetwork cascading effects are a response of networks to their dependence or interdependence. For utility networks, internetwork cascading effects commonly come from the dependence of utility-dependent equipment on utilities. In URCs, the dependence of routers and pumps on electricity are two typical examples. In factor analysis, the strength of these two types of cascading effects is taken as the variable of analysis, which is described using the dependence strength coefficient (i.e., $\alpha_{UC/SRa'}$).

Multidimensional resilience assessment system

Community performance indicator

To develop a more comprehensive indicator, the performance of URCs is shown from three perspectives herein: functionality, efficiency, and toughness. Existing studies often use the outputs of physical systems to define functionality. Herein, the relationship between the functioning of physical systems and the behavior of their users (e.g., communities and their residents) is further considered. On this basis, functionality is defined with the of behavioral feedback of residents. This new definition of functionality does not contradict the existing definitions since it is just an extension of the existing ones. Furthermore, this new definition expands the connotation of functionality from a single dimension (i.e., physical) to two dimensions (i.e., physical and social).

Specifically, functionality is defined as the capability of a URC to meet the daily needs of residents. The better functionality a URC has, the more residents will settle. Accordingly, a post-earthquake staying population (i.e., I_S) is adopted as the indicator of functionality. It is assumed that the residents who move out due to seismic damage will return and reoccupy with the recovery of the community. Thus, I_S is a variable about the time [i.e., $I_S(t)$]. $I_S(t)$ can be calculated by the POM population and the percentage of the population that participate in the SOM:

$$I_S(t) = \left[I_T - I_{POM}(t)\right]\left[1 - i_{SOM}(t)\right] \tag{14}$$

where, I_T represents the initial total population of a community; $i_{SOM}(t)$, the population percentage of SOM, can be calculated by Eqn. (17); and $I_{POM}(t)$, the POM population of the community, can be calculated by the sum of the POM population of each residential building:

$$I_{POM}(t) = \sum_{g=1}^{N_{RB}} I_{RB_g,POM}(t) = \sum_{g=1}^{N_{RB}} \left[I_{RB_g,T} - I_{RB_g,S}(t)\right] \tag{15}$$

where, N_{RB} is the number of residential buildings; the subscript, RB_g, represents the g^{th} residential building; $I_{RBg,POM}(t)$, the POM population of RB_g, is equal to the difference between the total population of RB_g (i.e., $I_{RBg,T}$) and its post-earthquake staying population [i.e., $I_{RBg,S}(t)$]. Because the residents moved out due to seismic damages of residential buildings will return with the recovery, $I_{RBg,S}(t)$ and $I_{RBg,POM}(t)$ will change with t.

Because residents are allowed to occupy a building only when it is occupiable or fully functional, $I_{RB,S}(t)$ can be calculated by the expected value of the staying population of these two functional states:

$$I_{RB,S}(t) = P_{RB,O}(t) I_{RB,O} + P_{RB,F}(t) I_{RB,F} \quad (16)$$

where, $P_{RB,F}(t)$ and $P_{RB,O}(t)$ are the probabilities of the occupiable state and fully functional state respectively. They can be calculated by Eqns. (4)~(5). $I_{RB,O}$ and $I_{RB,F}$ represent the numbers of people living in the building when it is occupiable and fully functional respectively. The values of $I_{RB,O}$ and $I_{RB,F}$ mainly depend on the risk appetite of residents and their requirements for the quality of life.

If the dependent attitudes of residents are not sensitive to the negative influences caused by neighborhood damages, it can be assumed that the outmigration will be barely affected by neighborhood damages. Based on this assumption, few residents will choose to move out when a residential building is fully functional. Thus, $I_{RB,F}$ is approximately equal to $I_{RB,T}$ in this case. However, the effects of neighborhood damages on outmigration should be further considered if residents are sensitive to this factor. Otherwise, there will be a risk of underestimating the outmigration. If a more accurate outmigration quantification is required, the EPUB decision model presented by Burton et al. (2019) will be recommended to assess the influences caused by neighborhood damages. When a residential building is in the occupiable state, whether its residents move out or not primarily depends on their dependent attitudes. For the convenience of calculation, the outmigration probability was assumed to be 0% (Burton et al. 2016). This implies that all residents will continue to live in a building that is occupiable but dysfunctional. However, this assumption is not applicable to densely populated URCs whose residents have diverse attitudes. To describe the outmigration more credibly, $I_{RB,O}$ is assumed to be 50% of $I_{RB,T}$ in this study. This means that half of the residents will choose to continue living when their residential buildings are just occupiable.

Similarly, $i_{SOM}(t)$ of Eqn. (14) can be calculated using the expected SOM population percentage of different combinations of functional states of supporting buildings:

$$i_{SOM}\left(t\right)=\sum_{p=1}^{N_{SBF,SBDF}}\left[i_{SBF_p,SBDF_p,SOM}\prod\nolimits_{SB_h\in SBF_p}P_{SB_h,F}\left(t\right)\prod\nolimits_{SB_{h'}\in SBDF_p}P_{SB_{h'},DF}\left(t\right)\right] \quad (17)$$

where, $N_{SBF,SBDF}$ is the number of combinations of functional states of supporting buildings. The subscripts, SBF_p and $SBDF_p$, respectively denote the collections of functional and dysfunctional supporting buildings in the p^{th} combination. $i_{SBFp,SBDFp,SOM}$, the SOM population percentage of the p^{th} combination, can be calculated by data obtained from residential satisfaction surveys. SB_h and $SB_{h'}$ are the h^{th} and h'^{th} supporting buildings in SBF_p and $SBDF_p$ respectively. The functioning probability of SB_h [i.e., $P_{SBh,F}(t)$] and the dysfunctional probability of $SB_{h'}$ [i.e., $P_{SBh',DF}(t)$] can be calculated by Eqn. (4). Eqn. (17) can be specifically written as Eqn. (18) for the supporting buildings concerned in this study:

$$\begin{aligned} i_{SOM}\left(t\right)=\ & P_{EB,F}\left(t\right)P_{CB,F}\left(t\right)P_{MB,F}\left(t\right)i_{\{EB,CB,MB\},\varnothing,SOM}+P_{EB,F}\left(t\right)P_{CB,F}\left(t\right)P_{MB,DF}\left(t\right)i_{\{EB,CB\},\{MB\},SOM}+\\ & P_{EB,F}\left(t\right)P_{CB,DF}\left(t\right)P_{MB,F}\left(t\right)i_{\{EB,MB\},\{CB\},SOM}+P_{EB,DF}\left(t\right)P_{CB,F}\left(t\right)P_{MB,F}\left(t\right)i_{\{CB,MB\},\{EB\}SOM}+\\ & P_{EB,F}\left(t\right)P_{CB,DF}\left(t\right)P_{MB,DF}\left(t\right)i_{\{EB\},\{CB,MB\},SOM}+P_{EB,DF}\left(t\right)P_{CB,F}\left(t\right)P_{MB,DF}\left(t\right)i_{\{CB\},\{EB,MB\},SOM}+\\ & P_{EB,DF}\left(t\right)P_{CB,DF}\left(t\right)P_{MB,F}\left(t\right)i_{\{MB\},\{EB,CB\},SOM}+P_{EB,DF}\left(t\right)P_{CB,DF}\left(t\right)P_{MB,DF}\left(t\right)i_{\varnothing,\{EB,CB,MB\},SOM} \end{aligned}$$

(18)

where, the subscripts, EB, CB, and MB, represent the buildings used for education, commercial retail, and medical care respectively. In addition, if all of the supporting buildings function normally, the SOM population percentage will be 0 (i.e., $i_{\{EB,CB,MB\},Ø,SOM}=0$).

The concept of toughness is similar to the concept of robustness. In the research field of resilience, robustness is commonly understood as the ability of elements and systems to withstand a given level of stress without suffering degradation or loss of function (Bruneau et al. 2003). Robustness is a static indicator that only describes the state of a system at a certain moment, while the performance indicators employed herein need to be dynamic indicators that can reflect the time-varying property of community recovery. In order to emphasize the dynamic characteristics, the concept of toughness is proposed to distinguish it from robustness. Specifically, toughness is a dynamic indicator that describes the ability of a system to dynamically maintain its original functionality after perturbation. In order to consider the topological characteristics of infrastructural networks concerned in this study, toughness is indicated using a node connectivity function with time as its independent variable. Node connectivity (Boccaletti et al. 2006), a classic indicator describing the ability of nodes in a network to maintain their connections under perturbations, is typically defined as the average of the degrees of all nodes in a network.

Although the utilities transported by the networks are different, all of these networks can be regarded of as source-sink networks mathematically. The concept of source-sink has already been widely used in investigating different types of utility networks (Kowalski et al. 2019). Specifically, the source nodes represent the sources of the utilities (e.g., the upper-level utility networks), while the sink nodes represent the destinations of the utilities (e.g., the households). Because the functional states of utility networks primarily depend on the probability of source-sink connection, their toughness should be indicated by the probabilistic source-sink connectivity [i.e., $K_{UN}(t)$] instead of the general node connectivity. $K_{UN}(t)$ is defined as the average of the expected numbers of source-sink pathways owned by each sink node:

$$K_{UN}(t) = \left[\sum_{c=1}^{N_{SN}} \sum_{b=1}^{N_{SR}} PW_{SR_b \& SN_c}(t)\right] \Big/ N_{SN} \tag{19}$$

where, N_{SR} and N_{SN} are the number of source nodes and sink nodes respectively; $PW_{SRb\&SNc}(t)$ is the expected number of pathways connecting SN_c and SR_b. It can be calculated by:

$$PW_{SR_b \& SN_c}(t) = \sum_{d=1}^{N_{PW}} \left[P_{PW_d,P}(t) A_{PW_d}(t)\right] \tag{20}$$

where, N_{PW} is the number of pathways; PW_d stands for the d^{th} pathway; $P_{PWd,P}(t)$, the probability that PW_d is passable, can be calculated by Eqn. (2); and $A_{PWd}(t)$ is the adjacency variable of PW_d. When PW_d is passable, the value of $A_{PWd}(t)$ is 1, otherwise it is 0.

The concept of efficiency can be understood as an expression of how efficiently information or utilities are exchanged over the network (Latora and Marchiori 2001). The efficiency of a general network is usually described by the characteristic path length, graphics efficiency, and other topological indicators. Particularly, because graphics efficiency can avoid the divergence caused by disconnected components, this indicator has been widely used in studies about complex networks (Boccaletti et al.

2006). In order to highlight the influence of the fragilities of pipelines on the efficiency, the efficiency of a utility network (UN) [i.e., $U_{UN}(t)$] is defined as Eqn. (21) with reference to the concept of graphics efficiency:

$$U_{UN}(t)=1/PL_T(t) \tag{21}$$

where, $PL_T(t)$, the total probabilistic length of the UN, is defined as the sum of the probabilistic lengths of all related pipe sections:

$$PL_T(t)=\sum_{e=1}^{N_{PS}} PL_{PS_e}(t)=\sum_{e=1}^{N_{PS}}\left[L_{PS_e,P}/P_{PS_e,F}(t)\right] \tag{22}$$

where, N_{PS} is the number of sections of the pipe; PS_e represents the e^{th} section; and $PL_{PSe}(t)$, the probabilistic length of PS_e, is calculated by the physical length of PS_e (i.e., $L_{PSe,P}$) and its functioning probability [i.e., $P_{PSe,F}(t)$]. $P_{PSe,F}(t)$ can be calculated by Eqn. (3). To reflect the influence of seismic fragility on efficiency, probabilistic length instead of physical length is used herein.

If the importance of the four utility networks is assumed to be the same, the efficiency and toughness of the entire system of utility networks can be described using unweighted averages:

$$U(t)=\sum_{a=1}^{N_{UN}} U_{UN_a}(t)/N_{UN} \tag{23a}$$

$$K(t)=\sum_{a=1}^{N_{UN}} K_{UN_a}(t)/N_{UN} \tag{23b}$$

where, N_{UN} is the number of utility networks; and $U(t)$ and $K(t)$ represent the efficiency and toughness of the entire system of utility networks respectively. To highlight the relative development trends of the three types of performance, they are normalized by initial values:

$$i_S(t)=I_S(t)/I_S(0)=I_S(t)/I_T \tag{24a}$$

$$u(t) = U(t)/U(0) \tag{24b}$$

$$k(t) = K(t)/K(0) \tag{24c}$$

where, $i_s(t)$, $u(t)$, and $k(t)$, which are the normalized values of $I_s(t)$, $U(t)$, and $K(t)$ respectively, are taken as the performance indicators. $U(0)$ and $K(0)$ can be calculated by Eqn. (23) with t=0.

Seismic resilience metric

To comprehensively assess the recovery capacity of a URC, three types of metrics (i.e., loss-related metric, time-related metric, effectiveness-related metric) are used to quantify resilience from different perspectives. Loss-related metrics measure resilience using seismic losses (Rose 2007). In particular, cumulative loss is a classic loss-related metric (Bruneau et al. 2003) that can be calculated by the integral of a recovery curve:

$$R_L = \int_0^{t_{TRD}} \left[1 - C(t)\right] dt \tag{25}$$

where, R_L is the cumulative loss; $C(t)$, the generalized performance at time t, is a general term for $i_s(t)$, $u(t)$, and $k(t)$; t_{TRD}, the total recovery duration of the community, is numerically equal to the repair completion time of the basic component repaired at the last. Time-related metrics use temporal quantities to measure resilience from the perspective of rapidity (Cimellaro et al. 2010). The recovery period (i.e., R_T) is a time-related metric that describes the total time consumed by the repair process. Its value is equal to t_{TRD}:

$$R_T = t_{TRD} \tag{26}$$

Effectiveness-related metrics use the effect of recovery measures to characterize resilience. Herein, this effect is described by the resilience threshold (Tao and He 2020a):

$$R_E = \sqrt{8\left(p_1 + p_2 X_0 + p_3 / t_{TRD,norm}\right) / m} \tag{27}$$

where, R_E is the resilience threshold; X_0, the so-called initial inoperability, is equal to $1-Q(0)$; $t_{TRD,norm}$, the normalized recovery duration, can be calculated by the corresponding normalization approach (Tao and He 2020a); p_1, p_2, p_3, and m are the constant coefficients whose recommended values have been obtained by conducting a nonlinear fitting of 400 virtual community recovery cases (Tao and He 2020a). According to the original definition of Eqn. (27) (Tao and He 2020a), it is derived from a dynamics model describing community recovery. This dynamics model is a limit cycle which mathematically describes the maximum loss that a community can withstand when it adopts a resilience strategy with a certain cost. And, Eqn. (27) is an expression for this maximum loss. That is, when the seismic damage exceeds R_E, the community is unrecoverable (or, it is uneconomical to recover). Therefore, R_E is regarded as a metric of the resilience threshold of a community (Tao and He 2020a). The resilience threshold metric is selected because it can prevent the inadequacy of some existing metrics using dynamics methodology which can effectively capture the fundamental mechanism of community recovery.

These metrics and the above-mentioned performance indicators constitute a multidimensional resilience assessment framework (see Fig. 6). When this framework is used, it is unnecessary to use all of the indicators and metrics it contains. Instead, it is recommended to allocate these indicators and metrics flexibly in accordance with specific analysis needs. For example, if functionality degradation is the focus of research, community resilience is recommended to be assessed with the 7th combination (i.e., the cumulative loss of functionality). This framework provides a modular assessment system rather than an integrated assessment method. Because the metrics and indicators adopted herein can be applied to different kinds of disasters, this assessment framework is not only applicable to earthquake-induced damage scenarios but also other disasters.

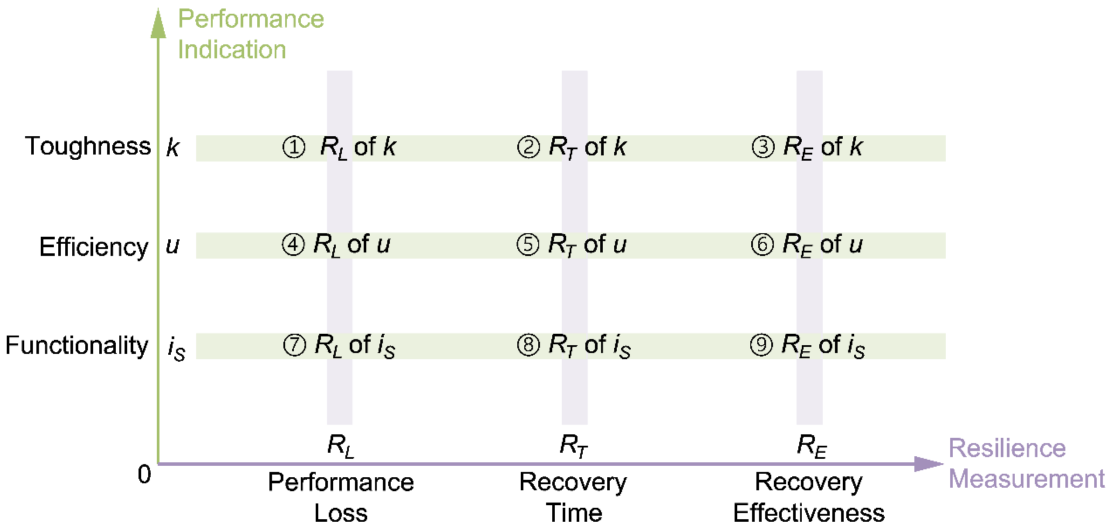

Note: R_E = Resilience threshold; R_L = Cumulative loss; R_T = Recovery period; i_S = Normalized functionality indicator; k = Normalized toughness indicator; u = Normalized efficiency indicator.

Fig. 6. Multidimensional resilience assessment framework

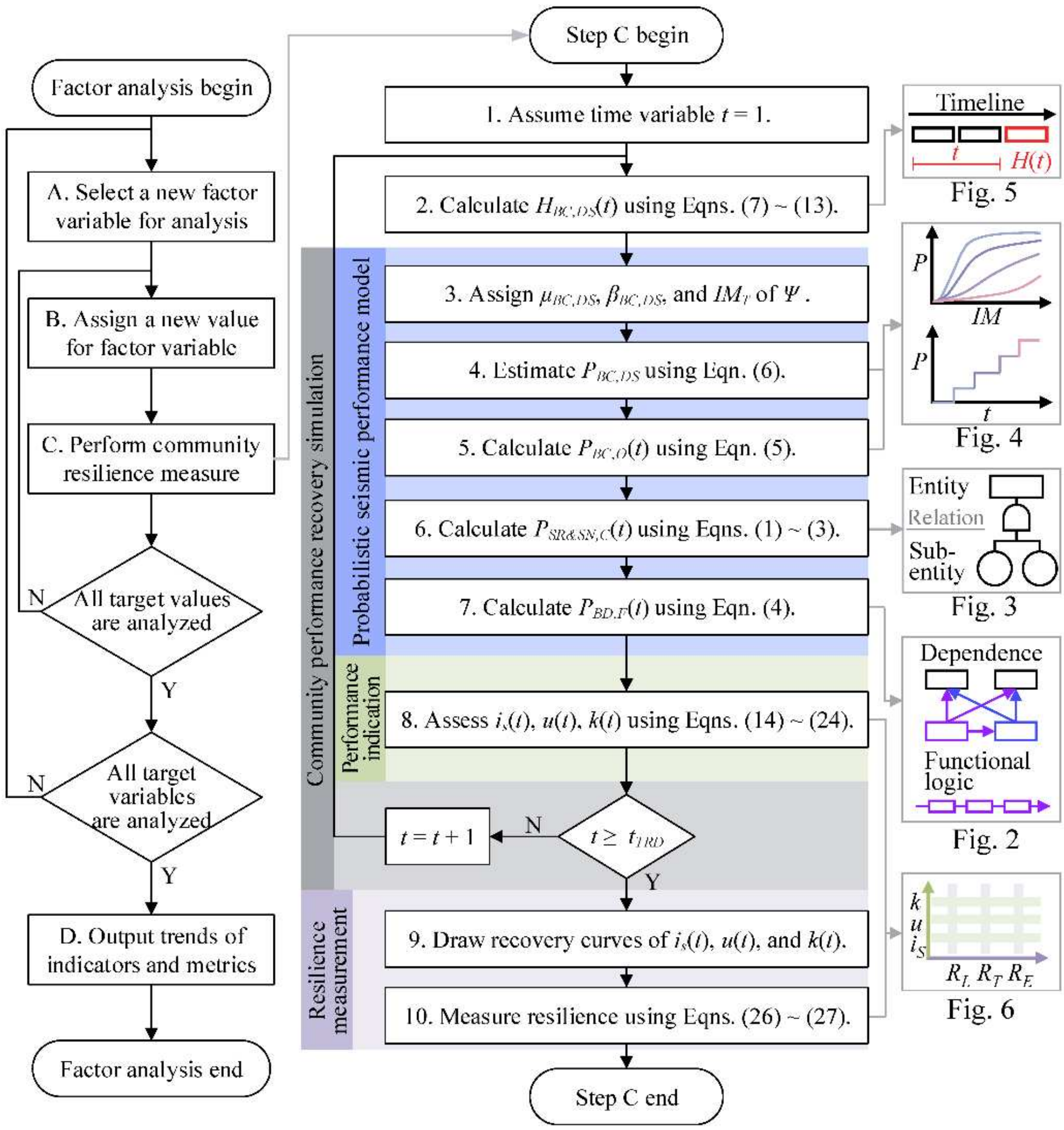

Fig. 7. Flowchart of resilience assessment and factor analysis

The impacts of infrastructural characteristics can be analyzed according to the process shown in Fig. 7. The process smoothly integrates infrastructural dependence analysis (see Figs. 2 and 3), seismic damage analysis (see Fig. 4), repair sequence description (see Fig. 5), and the multidimensional assessment framework (see Fig. 6) into a complete methodology for resilience assessment and factor analysis. This methodology provides a solution for comparing the impacts of different types of infrastructural characteristics on community recovery, which can lead to a more comprehensive and in-depth understanding of community resilience, resulting in helping community leaders and stakeholders formulate more efficient and reliable resilience improvement programs. Because the damage analysis (i.e., the 4th and 5th steps) is specialized to earthquake disasters, the probabilistic performance models built on it and even the whole methodology are only applicable to earthquake disasters, even though the proposed assessment framework can be applied to different disasters.

Case study

Basic information

The case-study community is a small-scale URC with 12 buildings. Although the scale of this community is small, it has more than 10,000 residents and multiple utility networks and buildings. Such small-scale URCs with high plot ratios are common in densely populated Chinese cities. To house more residents, some high-rise apartments have been built in this community as residential buildings. The master plan of the community and its infrastructural information are shown in Fig. 8(a)~(b). Actually, the case-study community is a simplified model abstracted from a real URC in China. This model preserves the topology and fragility information of buildings and utility networks of the original community. By capturing the primary characteristics of the infrastructural system, the reliability of the resilience assessment based on this model can be ensured. The establishment of more complex and realistic community scenarios may require other specialized analysis methods (e.g., detailed flow models for utility networks, collapse and collision simulations for buildings) which are beyond the main scope of this study (i.e., resilience assessment and analysis). For this reason, more complex community modeling is not considered herein.

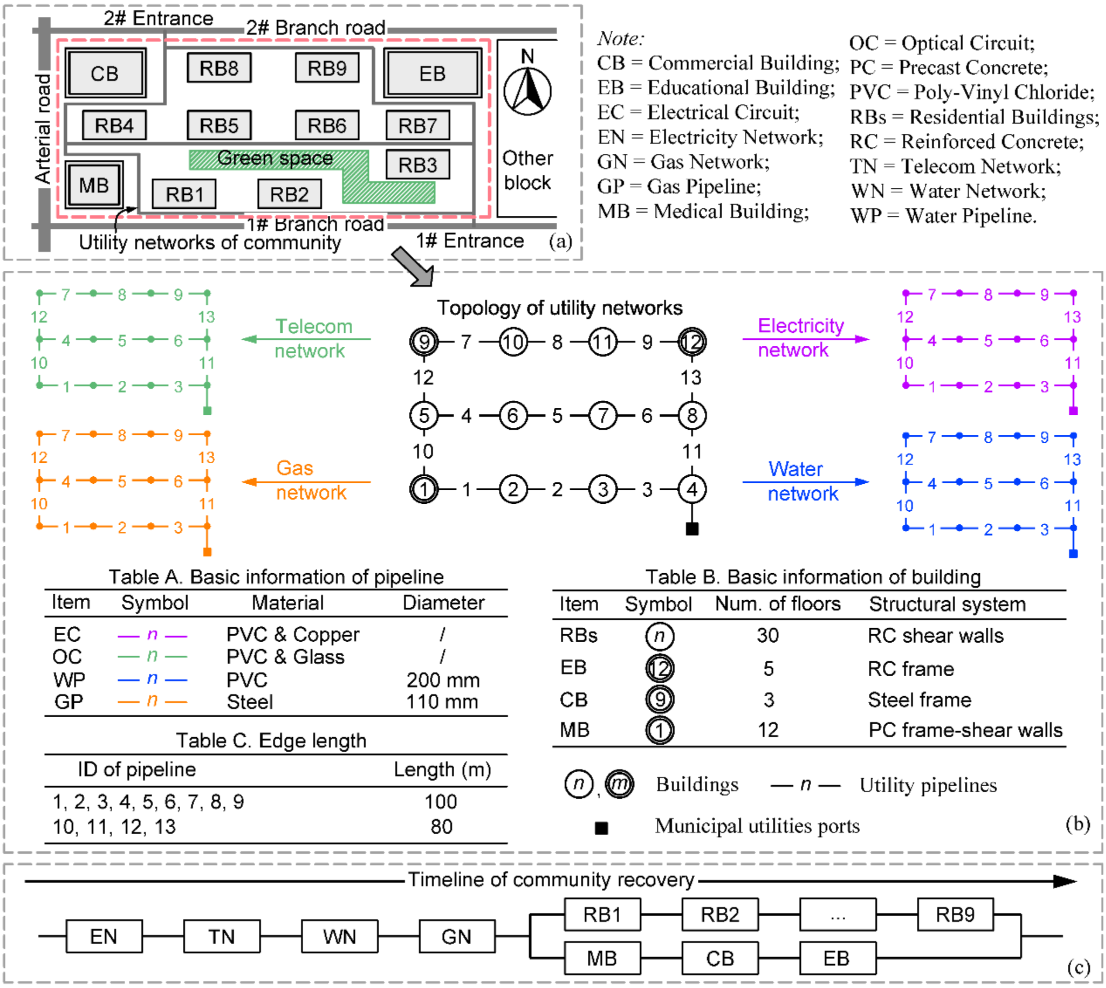

Fig. 8. Illustration of basic information of case community; (a) Community master plan; (b) Basic engineering information; (c) Default repair sequence

The seismic fragilities and recovery paths of the infrastructures are described by the aforementioned lognormal CDF [see Eqn. (6)] and step function [see Eqn. (7)] respectively. Based on the information shown in Fig. 8, the default values of the parameters can be obtained from the literature (see Table 1 and Table 2). The repair durations of utility networks are deliberately shortened in accordance with the fact that governments usually organize powerful construction forces to accelerate the repair of utility networks to provide conditions for other relief works. Because the recovery simulation method established above focuses on describing the randomness of infrastructural damages, time-related parameters are simply regarded as deterministic variables. Since the case-study community is small, the intensities of ground motions barely changes with the locations of different infrastructures. Thus, the targeted intensity is assumed to be 1000 gal for each infrastructure. In the default case, internetwork cascading effects are not considered (i.e., $\alpha_{TR/EN}$=0 and $\alpha_{WP/EN}$=0). The default infrastructural repair sequence is shown in Fig. 8(c).

If a residential building is assumed to provide 420 houses, and each house is occupied by a couple and a child, a single residential building and the entire community will accommodate 1,260 and 11,340 residents respectively. According to the above assumptions about $I_{RBg,F}$ and $I_{RBg,O}$, the proportion of residents who choose to continue to live is 100% and 50% respectively for fully functional residential buildings and occupiable residential buildings [see Eqn.(16)]. In this case, $I_{RBg,F}$ and $I_{RBg,O}$ are 1260 and 630 respectively. To describe the dependent attitudes of Chinese residents, the SOM population percentages are calculated using the residential satisfaction data of some Chinese URCs (see Table 3). The couplings in the SOM population percentages are estimated with the above-mentioned disability weightings (see Table 4), wherein the ratios of the disability weightings are ω_2/ω_1=1.82 and ω_3/ω_1=2.72 (Murray 1994).

Table 1. Values of parameters of fragility functions of basic components

Item	μ of PGA (g)				β of PGA (g)				Data source	Reference
	DS1	DS2	DS3	DS4	DS1	DS2	DS3	DS4		
RBs	0.12	0.23	0.57	1.07	0.64				Model C2H	(FEMA 2013)
EB	0.23	0.33	0.63	1.22	0.64				Model PC2H	
CB	0.16	0.28	0.60	1.27	0.64				Model S1L	
MB	0.15	0.25	0.60	1.30	0.64				Model C1M	
EC	0.24	0.33	0.58	0.89	0.25	0.20	0.15	0.15	Model EDC2	
OC	0.24	0.33	0.58	0.89	0.20	0.20	0.07	0.07	Model EDC2	
WP	*0.56*	*0.75*	*0.90*	*1.02*	*0.15*	*0.15*	*0.08*	*0.07*	Calculation	(Isoyama et al. 2000;
GP	*0.95*	*1.26*	*1.50*	*1.69*	*0.15*	*0.15*	*0.08*	*0.08*	Calculation	Loganathan et al. 2002)

Note: Underlined values come directly from references; *Values in italic type* are calculated from data provided by references; CB = Commercial Building; DS = Damage State; EB = Educational Building; EC = Electrical Circuit; GP = Gas Pipeline; MB = Medical Building; OC = Optical Circuit; PGA = Peak Ground Acceleration; RBs = Residential Buildings; WP = Water Pipeline; μ = Median of fragility function; β = Log-standard deviation of fragility function.

Table 2. Repair durations of basic components

Item	Repair duration (day)					Data source	Reference
	DS0	DS1	DS2	DS3	DS4		
RBs	*0*	*10.0*	*30.0*	*120.0*	*360.0*	Assumption	(Tao and He 2020b; MOHURD 2016)
EB	0	5.0	20.0	90.0	180.0	Model EFS1	(FEMA 2013)
CB	0	5.0	20.0	90.0	180.0	Model EDFLT	
MB	0	5.0	20.0	90.0	180.0	Model EFHS	
EC	*0*	*0.4*	*1.7*	*7.5*	*15.0*	Assumption	(MOHURD 1993)
OC	*0*	*0.4*	*1.7*	*7.5*	*15.0*	Assumption	
WP	*0*	*0.3*	*1.1*	*5.0*	*10.0*	Assumption	
GP	*0*	*0.5*	*2.2*	*9.9*	*19.8*	Assumption	

Note: Underlined values come directly from references; *Values in italic type* are assumed based on data provided by references.

The factor analysis consists of four parts (see Table 5): The first part is used in illustrating the importance of modeling repair sequences of different repair plans (i.e., RPs) (see Table 6). Specifically, the 1st repair plan (RP1) has the highest efficiency but requires more resources. The efficiency of the 2nd and 3rd repair plans (RP2 and RP3) are lower than it of RP1 but require fewer resources. Although the resources required by the 4th and 5th repair plans (RP4 and RP5) are similar to those of RP2 or RP3, they are rarely adopted in reality because their repair sequences are unreasonable. However, in order to compare different repair sequences, RP4 and RP5 are still considered herein. The latter three parts of the factor analysis are used to capture the effects of the three infrastructural characteristics. Changes in network topology are shown in Fig. 9.

Table 3. Secondary outmigration caused by a dysfunctional supporting building

No.	Item	Population percentage of secondary outmigration								
		CQ	WH1	WH2	QHD	DJY	YX	BC1	BC2	Avg.
I_0	$i_{\{EB,CB,MB\},\emptyset,SOM}$	N.A.	N.A.	N.A.	N.A.	N.A.	N.A.	N.A.	N.A.	**0**
I_1	$i_{\{CB,MB\},\{EB\},SOM}$	30.3%	25.2%	15.8%	27.7%	14.8%	16.5%	15.9%	18.9%	**20.6%**
I_2	$i_{\{EB,MB\},\{CB\},SOM}$	12.5%	19.3%	33.2%	33.0%	12.1%	13.6%	13.1%	12.6%	**18.7%**
I_3	$i_{\{EB,CB\},\{MB\},SOM}$	21.0%	28.7%	23.4%	26.9%	18.1%	16.6%	16.0%	18.9%	**21.2%**

Note: Avg. = Average; BC = Beichuan (Qiao 2013); CQ = Chongqing (Chen 2007); DJY = Dujiangyan (Qiao 2013); QHD = Qinghuangdao (Meng 2012); WH = Wuhan (Ma 2008; He and Yang 2011); YX = Yingxiu (Qiao 2013).

Table 4. Secondary outmigration caused by two or three dysfunctional supporting buildings

No.	Item	Formula	Population percentage
A_1	Avg. of I_1, I_2	$(I_1+I_2)/2$	19.7%
A_2	Avg. of I_1, I_3	$(I_1+I_3)/2$	20.9%
A_3	Avg. of I_2, I_3	$(I_2+I_3)/2$	20.0%
A_4	Avg. of I_1, I_2, I_3	$(I_1+I_2+I_3)/3$	20.2%
I_4	$i_{\{MB\},\{EB,CB\},SOM}$	$A_1\times\omega_2/\omega_1$	**35.7%**
I_5	$i_{\{CB\},\{EB,MB\},SOM}$	$A_2\times\omega_2/\omega_1$	**38.0%**
I_6	$i_{\{EB\},\{CB,MB\},SOM}$	$A_3\times\omega_2/\omega_1$	**36.3%**
I_7	$i_{\emptyset,\{EB,CB,MB\},SOM}$	$A_4\times\omega_3/\omega_1$	**55.1%**

Table 5. Variable information in factor analysis

Factor	Variable	Change in method or parameter value	
		Default	Modified
1. Repair sequence	$t_{BCi,j,k,RS}$	Calculating according to RP1	Calculating according to RP2, RP3, RP4, RP5 (see Table 6)
2. Seismic fragility (see Table.1)	$\mu_{UNs,DSs}$	$\mu_{UNs,DSs}\times1.0$	$\mu_{UNs,DSs}\times1.1, 1.2, 1.3, 1.4, 1.5$
	$\mu_{RBs,DSs}$	$\mu_{RBs,DSs}\times1.0$	$\mu_{RBs,DSs}\times1.1, 1.2, 1.3, 1.4, 1.5$
3. Topological redundancy	γ_U	$\gamma_U = 2$	$\gamma_U = 0, 1, 3, 4, 5, 6$ (see Fig. 10)
4. Internetwork cascading strength	$\alpha_{TR/EN}$	$\alpha_{TR/EN} = 0$	$\alpha_{TR/EN} = 0.2, 0.4, 0.6, 0.8, 1.0$
	$\alpha_{WP/EN}$	$\alpha_{WP/EN} = 0$	$\alpha_{WP/EN} = 0.2, 0.4, 0.6, 0.8, 1.0$

Note: RP = Repair Plan; $t_{BCi,j,k,RS}$ = Repair start time of $BC_{i,j,k}$; $\alpha_{TR/EN}$, $\alpha_{WP/EN}$ = Dependence strength coefficients of telecommunication routers and water pumps on electricity network; γ_U = Topological redundancy; $\mu_{UNs,DSs}$, $\mu_{RBs,DSs}$ = Medians of fragility functions of utility networks and residential buildings.

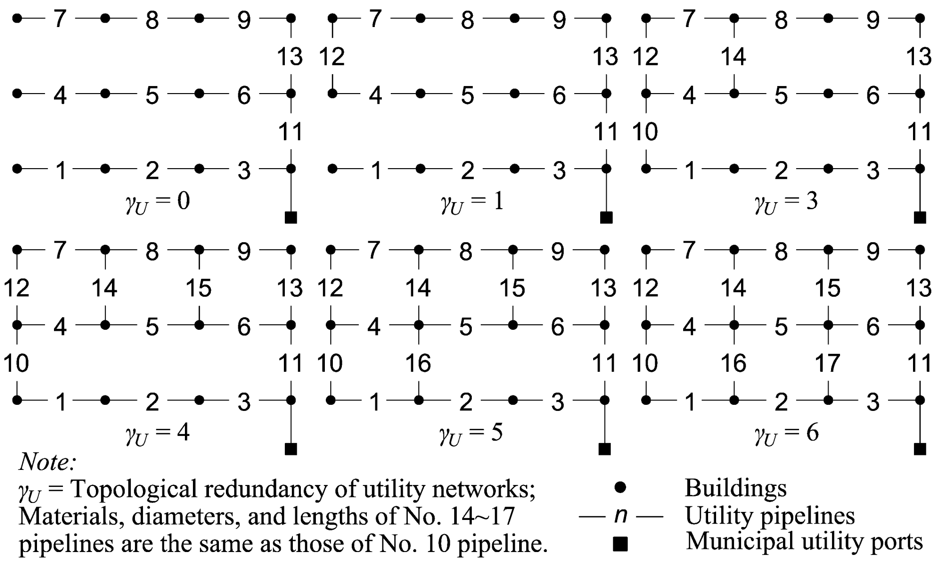

Fig. 9. Changes in topology of utility networks

Table 6. Changes in repair sequence of facility groups in factor analysis

Repair Plan (RP)	First	Second	Third
1	UNs	RBs & SBs	/
2	UNs	RBs	SBs
3	UNs	SBs	RBs
4	RBs	UNs	SBs
5	RBs	SBs	UNs

Note: UNs = Utility networks; RBs = Residential buildings; SBs = Supporting buildings.

Analysis results and discussion

Changes in repair sequences can significantly affect the recovery of functionality [see Fig. 10(a)]. Specifically, RP1 has the highest efficiency since the two types of buildings are repaired simultaneously. Both RP2 and RP3 show steadily rising recovery curves with similar recovery periods. The cumulative loss of RP2 is less than that of RP3, because RP2 prioritizes the repair of residential buildings so that the residents that can accept the dysfunction of supporting buildings can reoccupy earlier. Because the delay of repairs of utility networks affects the functioning of buildings, the recovery curves of RP4 and RP5 rise slowly.

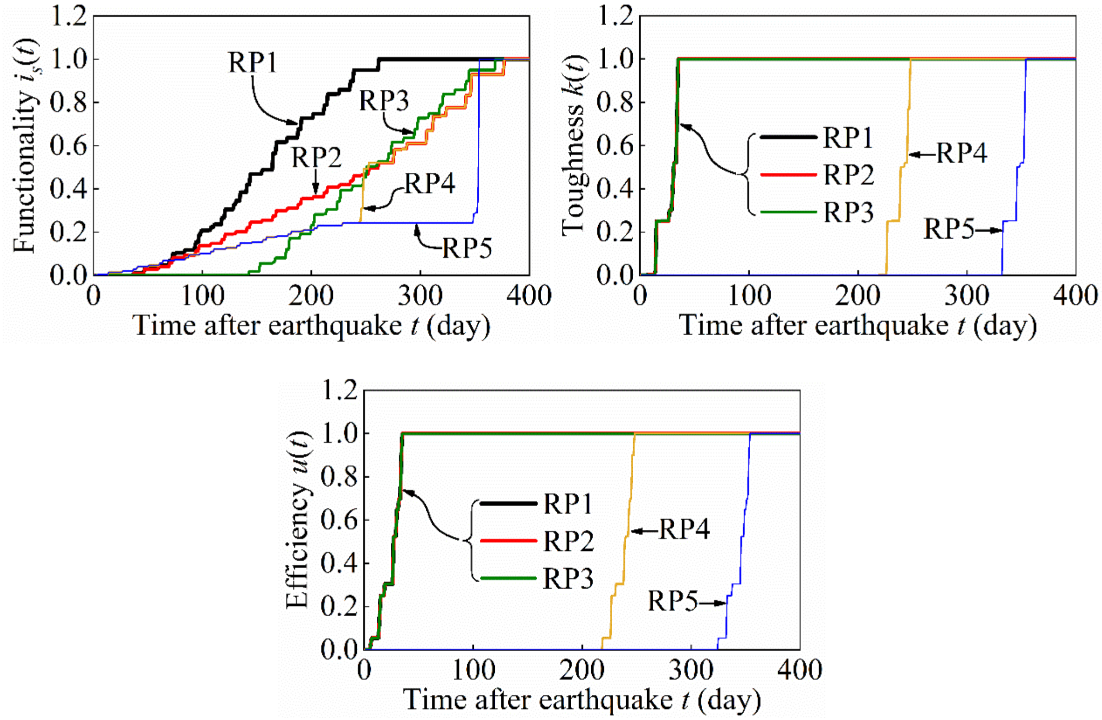

Fig. 10. Development trends of performance indicators under different repair plans; (a) Functionality; (b) Toughness; (c) Efficiency

Changes in the repair sequence of buildings (i.e., RP1~RP3) do not affect the recovery of toughness and efficiency [see Fig. 10(b)~(c)], because these two indicators which primarily depend on infrastructural topology are unrelated to the functionality of buildings. In addition, the delay of repairs of utility networks shifts the recovery curves of toughness and efficiency to the right without changing their shapes. According to Fig. 10, it is sensible to repair utility networks first, because this sequence can markedly reduce the recovery period and cumulative losses of the three indicators.

The functionality recovery curve shifts to the left as the seismic performance of utility networks improves [see Fig. 11(a)], because the reduction of their seismic damages advances the recovery process of the community. Correspondingly, this change raises the resilience threshold [see Fig. 11(e)], and reduces the cumulative loss and recovery period [see Fig. 11(c)~(d)]. However, changes in the metrics gradually slow down with the increase of $\mu_{\mathrm{UNs,DSs}}$. It can be inferred that the metrics will stop changing when $\mu_{\mathrm{UNs,DSs}}$ increases to a certain value. The effect of improving the seismic performance of utility networks on promoting functionality recovery is thus limited.

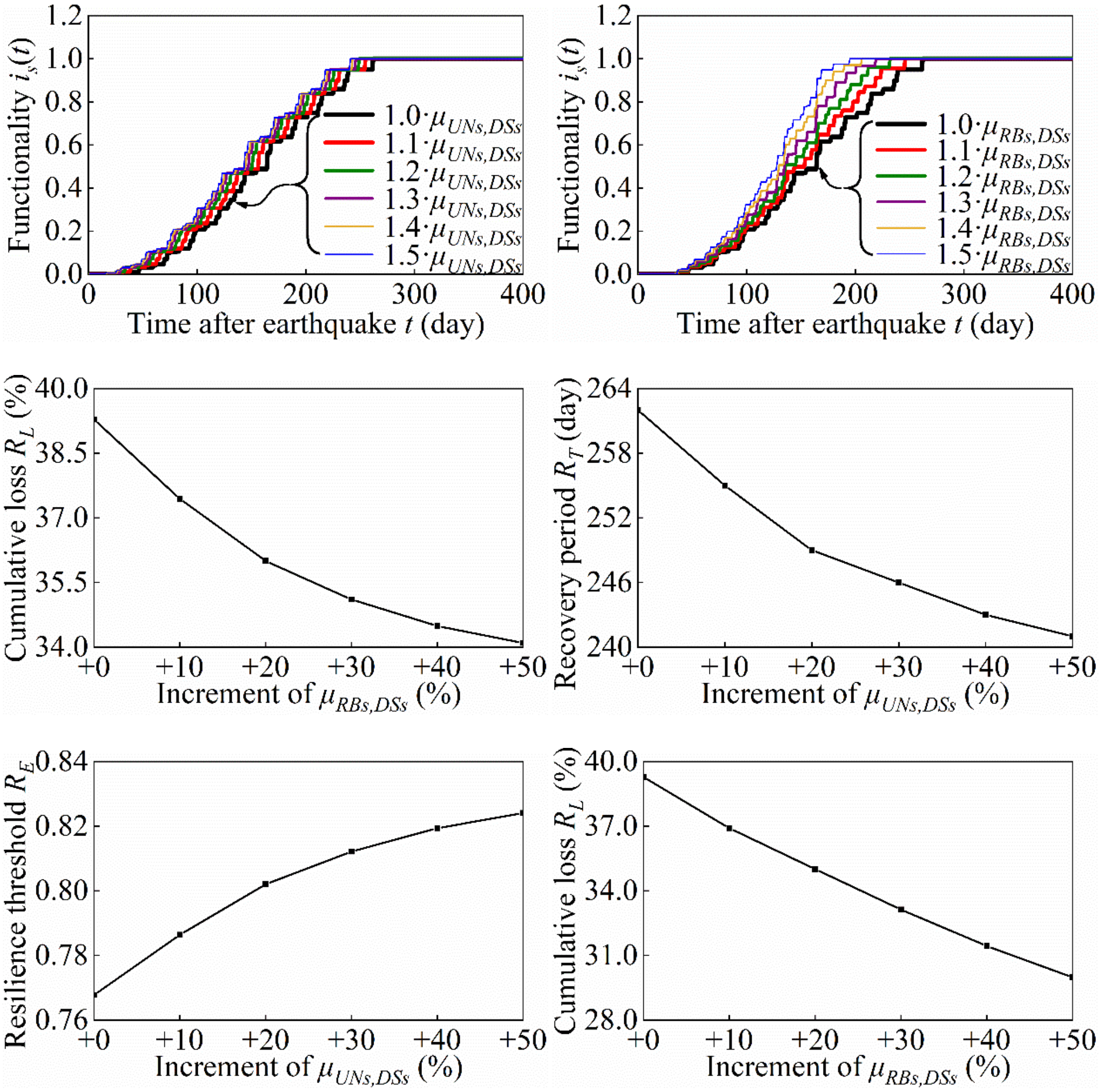

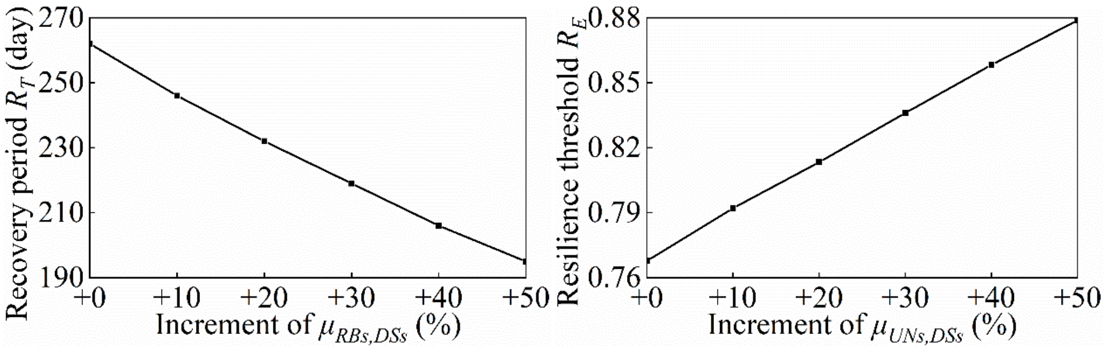

Fig. 11. Impacts of seismic fragility of utility networks and residential buildings on functionality; (a) Recovery curves (changing $\mu_{\mathrm{UNs,DSs}}$); (b) Recovery curves (changing $\mu_{\mathrm{RBs,DSs}}$); (c) Cumulative loss (changing $\mu_{\mathrm{UNs,DSs}}$); (d) Recovery period (changing $\mu_{\mathrm{UNs,DSs}}$); (e) Resilience threshold (changing $\mu_{\mathrm{UNs,DSs}}$); (f) Cumulative loss (changing $\mu_{\mathrm{RBs,DSs}}$); (g) Recovery period (changing $\mu_{\mathrm{RBs,DSs}}$); (h) Resilience threshold (changing $\mu_{\mathrm{RBs,DSs}}$)

The rising section of the functionality recovery curve rotates anticlockwise around its starting point as the seismic performance of residential buildings improves [see Fig. 11(b)], because the reduction of their seismic damages significantly accelerates the recovery process of the community. Thus, the resilience threshold increases [see Fig. 11(g)], while the cumulative loss and recovery period decrease [see Fig. 11(f)~(g)]. The metrics change linearly with the increase in $\mu_{\mathrm{UNs,DSs}}$. By comparison, it is found that the functionality recovery is better promoted by improving the seismic performance of residential buildings than utility networks. This phenomenon may be caused by the fact that the residential space provided by residential buildings is more important to the occupancy of residents than the utilities provided by utility networks. Because residential space is commonly more fundamental than utilities for the living of residents, the explanation obtained for the case-study community can be extended to most typical urban residential communities.

Besides, the changes in toughness and efficiency whose definitions are only related to infrastructural topology are no longer shown in Fig. 11.

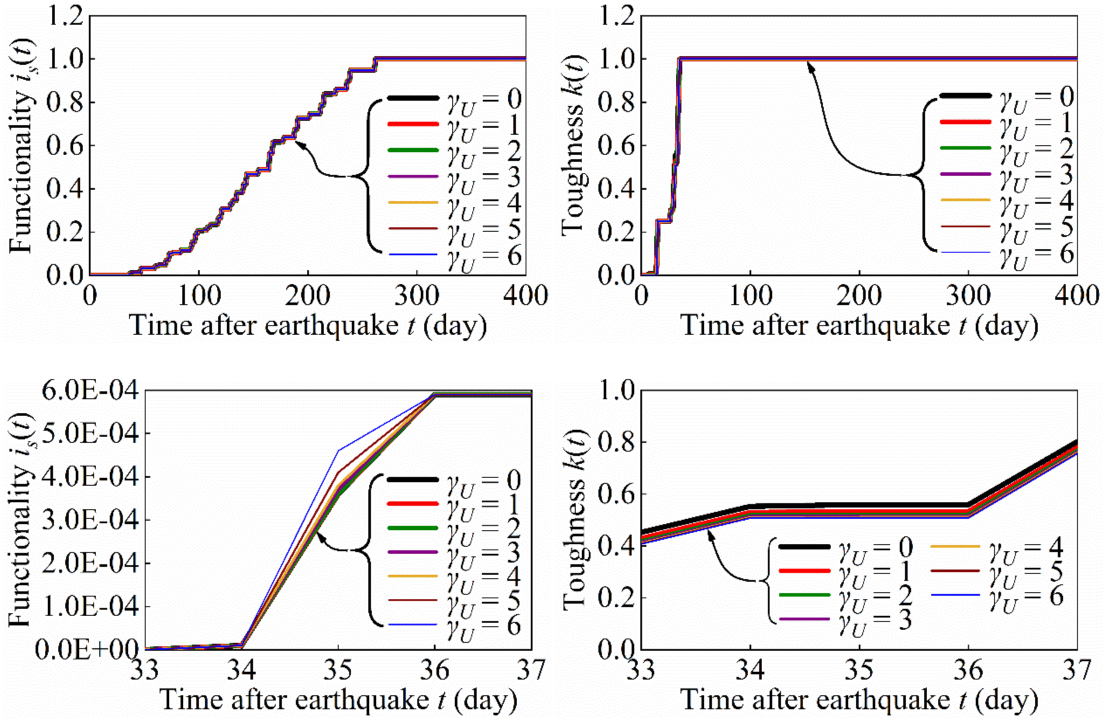

Fig. 12. Impacts of topological redundancy of utility networks on the recovery of functionality and toughness; (a) Functionality recovery curve; (b) Toughness recovery curve; (c) Functionality recovery curve (the 33th~37th days); (d) Toughness recovery curve (the 33th~37th days)

Changes in topological redundancy appear to be ineffective in promoting the recovery of functionality and toughness [see Fig. 12(a)~(b)]. However, after narrowing the scope of the time axis, small increases are shown [see Fig. 12(c)~(d)]. Obviously, changes in γ_U do affect the recoveries of functionality and toughness, but its effect and duration are limited. This result is caused by two factors: (1) a few redundant pipelines can hardly change the recovery of the case-study community; (2) the repair duration of utility networks is much shorter than that of the entire community. Besides, the curve of efficiency is not shown in Fig. 12 because it does not change with topological redundancy. Although topological redundancy has little effect on the recovery of the case-study community, this factor should not be ignored since it may cause a stronger impact in some URCs whose repair processes take longer time.

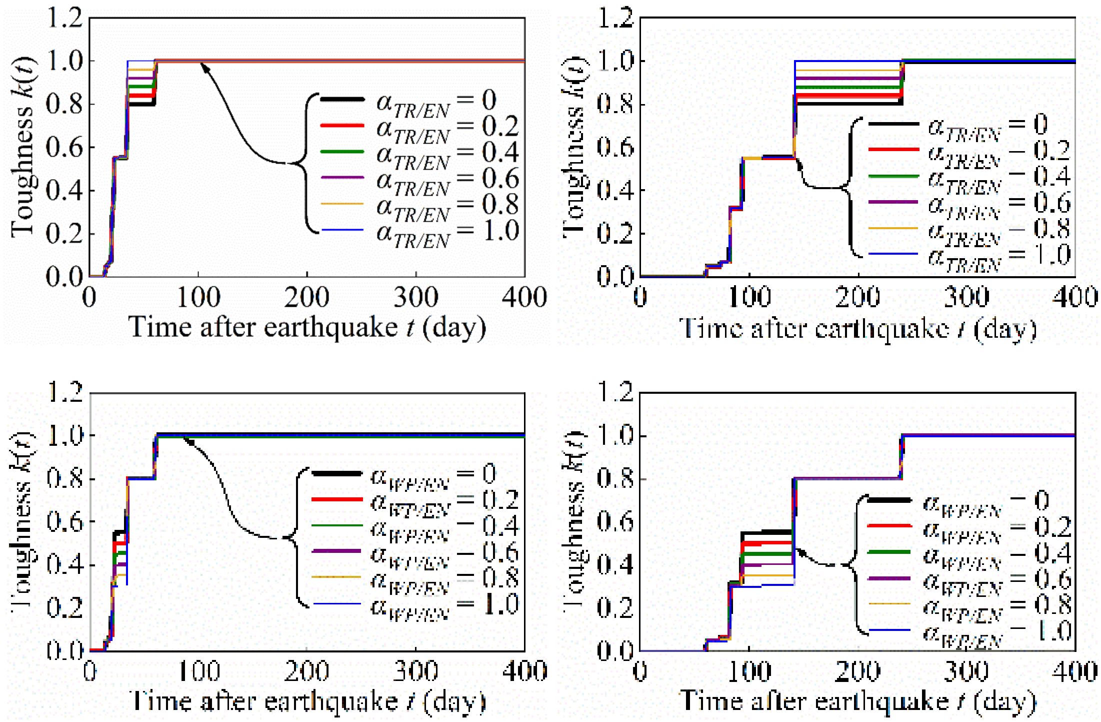

Fig. 13. Impacts of internetwork cascading effects of utility networks on toughness recovery; (a) Toughness recovery curve ($\alpha_{TR/EN}$, normal); (b) Toughness recovery curve ($\alpha_{WP/EN}$, normal); (c) Toughness recovery curve ($\alpha_{TR/EN}$, decelerated); (d) Toughness recovery curve ($\alpha_{WP/EN}$, decelerated)

For routers with independent direct current supply, the additional electricity power provided by the electricity network can reduce their dysfunctional risks caused by power outages. Therefore, the increase in the dependence of telecom routers on electricity networks promotes the recovery of toughness [see Fig. 13(a)]. In contrast, if water pumps are additionally installed, the recovery curve of toughness will decrease as the dependence of pumps on electricity increases [see Fig. 13(b)], because this dependence may increase the risk of water shortage due to the possible seismic damage of the electricity network. Obviously, the influences of internetwork cascading effects can be positive or negative; thus, it should not be simply assumed that community resilience can be improved by increasing or decreasing internetwork cascading effects before investigating the dependence mode of devices on utilities.

Moreover, if the recovery is decelerated, the duration of the cascading effects will be prolonged [see Fig. 13(c)~(d)]. The duration of cascading effects is thus closely related to the duration of repairing utility networks. According to Fig. 13, it can be seen that the proposed simulation method provides a direct way to characterize the internetwork cascading effects that exist in URCs. The curves of functionality and efficiency are not shown in Fig. 13 because their recoveries are barely affected by internetwork cascading effects. Although the scale of the case-study community is limited, various infrastructure-related and resident-related factors are exhaustively considered in this case study. Therefore, the results obtained from this small case-study community can also provide valuable references for subsequent studies on other larger communities.

Conclusions

(1) The key innovative contribution of this study is to systematically incorporate a series of analysis tools (e.g., seismic damage analysis, post-earthquake recovery

simulation, infrastructural dependence analysis, and population-based functionality indicator) into a comprehensive methodology for resilience assessment and analysis. Unlike existing studies that focus on the independent analyses of individual factors, the proposed methodology prefers to simultaneously investigate and compare the impacts of different types of factors using a unified standard from the perspective of URCs. This methodology can help the leaders and stakeholders of a URC understand the community resilience more comprehensively, resulting in developing more efficient and reliable resilience improvement programs.

(2) Based on the functionality indicators which can capture the infrastructural dependence in detail, as well as the model of densely populated URCs consisting of multiple supporting buildings, utility networks, and residential buildings, this study quantifies the capability of a densely populated residential community to serve its residents after earthquakes in a more detailed way than existing studies. In addition, a specialized description method of infrastructural repair sequences is also proposed for urban residential communities. This method provides the possibility to flexibly depict various possible repair plans in community recovery simulation.

(3) Improvements in the seismic performance of utility networks and residential buildings can facilitate community recovery. As seismic performance improves, the impact of the former one will gradually diminish, while the impact of the latter one will remain basically unchanged. This difference implies that the residential space provided by residential buildings has a stronger impact on resident occupancy than the utilities provided by the utility networks. This phenomenon is likely to occur in most

typical URCs where residential space is treated as the most foundational element of resident living. As a better choice to facilitate the recovery of such communities, the improvement of the seismic performance of residential buildings needs to be given sufficient attention.

(4) The results of the case study show that the impacts of internetwork cascading effects may be positive or negative. Therefore, it should not be simply assumed that community resilience can be improved by increasing or decreasing the internetwork cascading effects. On the other hand, the addition or removal of a few redundant pipelines shows little impact on the recovery of the case-study community because the repair durations of the utility networks are short. However, in some practical situations where the repairs of utility networks are time-consuming, more attention should be given to these two factors, because their impacts will expand with the extension of those repair durations.

(5) Although the proposed recovery simulation method can describe the randomness of the seismic damages of infrastructures, it does not consider the randomness of repair durations. A systematic investigation of the statistical characteristics of repair durations is still urgently needed. The lack of consideration of transportation networks may make the simulation results more optimistic than actual situation. Although this difference is unobvious for the concerned URCs, transportation networks should still be incorporated in the future to obtain more realistic simulation results. Damage analysis methods for different kinds of disasters should also be incorporated into the proposed methodology to further expand the

scope of its application. In addition, the repair sequence function needs improving in the future to consider other types of repair processes, such as the flow repetitive construction operation which is common in actual construction projects.

Acknowledgements

This work was financially supported by the Fundamental Research Funds for the Central Universities (Grant No. DUT19G208).

References:

Almufti, I., Willford, M. (2013). REDi™ rating system: Resilience-based earthquake design initiative for the next generation of buildings. San Francisco, C.A., USA: Arup.

Boccaletti, S., Latora, V., Moreno, Y., Chavez, M., Hwang, D. U. (2006). Complex networks: Structure and dynamics. *Physics Reports*, 424(4-5), 175-308.

Bruneau, M., Chang, S. E., Eguchi, R. T., Lee, G. C., O'Rourke, T. D., Reinhorn, A. M., et al. (2003). A framework to quantitatively assess and enhance the seismic resilience of communities. *Earthquake Spectra*, 19(4), 733-752.

Burton, H. V., Deierlein, G., Lallemant, D., Lin, T. (2016). Framework for incorporating probabilistic building performance in the assessment of community seismic resilience. *Journal of Structural Engineering*, 142(8), C4015007.

Burton, H. V., Kang, H., Miles, S., Nejat, A., Yi, Z. (2019). A framework and case study for integrating household decision-making into post-earthquake recovery models. *International Journal of Disaster Risk Reduction*, 37, 101167.

Cai, H., Lam, N. S. N., Qiang, Y., Zou, L., Correll, R. M., Mihunov, V. (2018). A synthesis of disaster resilience measurement methods and indices. *International Journal of Disaster Risk Reduction*, 31, 844-855.

Cantelmi, R., Di Gravio, G., Patriarca, R. (2021). Reviewing qualitative research approaches in the context of critical infrastructure resilience. *Environment Systems and Decisions*, 41(3), 341-376.

Chang, S. E., Svekla, W. D., Shinozuka, M. (2002). Linking infrastructure and urban economy: Simulation of water-disruption impacts in earthquakes. *Environment and Planning B: Planning and Design*, 29(2), 281-301.

Chen, X. W. (2007). Discussion on urban residential community public service evaluation index system. Master Dissertation of Chongqing University. Chongqing, China (In Chinese).

Cimellaro, G. P., Reinhorn, A. M., Bruneau, M. (2010). Seismic resilience of a hospital system. *Structure and Infrastructure Engineering*, 6(1-2), 127-144.

Cutter, S. L., Burton, C. G., Emrich, C. T. (2010). Disaster resilience indicators for benchmarking baseline conditions. *Journal of Homeland Security and Emergency Management*, 7(1).

Dueñas-Osorio, L., Craig, J. I., Goodno, B. J. (2007). Seismic response of critical interdependent networks. *Earthquake Engineering and Structural Dynamics*, 36(2), 285-306.

Feng, K. R., Wang, N. Y., Li, Q. W., Lin, P. H. (2017). Measuring and enhancing resilience of building portfolios considering the functional interdependence among community sectors. *Structural Safety*, 66, 118-126.

Federal Emergency Management Agency (FEMA). (2013). Hazus-MH 2.1: Technical manual. Multi-hazard loss estimation methodology, earthquake model. Washington, D.C.

Federal Emergency Management Agency (FEMA). (2012). Seismic performance assessment of buildings (Report No.: FEMA P-58). Washington, D.C.

Freddi, F., Galasso, C., Cremen, G., Dall'Asta, A., Sarno, L. D., Giaralis, A., Gutiérrez-Urzúa, F., et al. (2021). Innovations in earthquake risk reduction for resilience: Recent advances and challenges. *International journal of disaster risk reduction*, 60, 102267.

Gifford R. (2007). Environmental psychology: Principles and practice. Coleville, W.A.: Optimal books, 1-25.

He, L. H., Yang, C. Q. (2011). Housing satisfaction of urban residents and its influential factors. *Journal of Public Management*, 8(2), 43-51 (In Chinese).

Isoyama, R., Ishida, E., Yune, K., Shirozu, T. (2000). Seismic damage estimation procedure for water supply pipelines. *Water Supply*, 18(3), 63-68.

Koliou, M., van de Lindt, J. W., McAllister, T. P., Ellingwood, B. R., Dillard, M., Cutler, H. (2020). State of the research in community resilience: progress and challenges. *Sustainable and Resilient Infrastructure*, 5(3), 131-151.

Kowalski, D., Kowalska, B., Bławucki, T., Suchorab, P., Gaska, K. (2019). Impact assessment of distribution network layout on the reliability of water delivery. Water, 11(3), 480.

Latora, V., Marchiori, M. (2001). Efficient behavior of small-world networks. *Physical review letters*, 87(19), 198701.

Loganathan, G. V., Park, S., Sherali, H. D. (2002). Threshold break rate for pipeline replacement in water distribution systems. *Journal of Water Resources Planning and Management*, 128(4), 271-279.

Ma, J. (2008). Study on the evaluation of urban resident housing quality satisfaction. Master Dissertation of Huazhong Agricultural University. Wuhan, Hubei, China (In Chinese).

Masoomi, H., van de Lindt, J. W., Peek, L. (2018). Quantifying socioeconomic impact of a tornado by estimating population outmigration as a resilience metric at the community level. *Journal of structural engineering*, 144(5), 04018034.

Meng, Y. Y. (2012). City livable community comprehensive evaluation and its application research. Master Dissertation of Yanshan University. Qinghuangdao, Hebei, China (In Chinese).

Miles, S. B., Burton, H. V., Kang, H. (2019). Community of practice for modeling disaster recovery. *Natural Hazards Review*, 20(1), 04018023.

Ministry of Housing and Urban-Rural Development (MOHURD). (1993). National municipal construction time quota. Beijing, China (In Chinese).

Ministry of Housing and Urban-Rural Development (MOHURD). (2016). Construction and installation time quota. (Report No.: TY01-89-2016). Beijing, China (In Chinese).

Murray, C. J. (1994). Quantifying the burden of disease: the technical basis for disability-adjusted life years. *Bulletin of the World Health Organization*, 72(3), 429-445.

Nejat, A., Ghosh, S. (2016). LASSO model of postdisaster housing recovery: Case study of Hurricane Sandy. *Natural Hazards Review*, 17(3), 04016007.

Ouyang, M., Dueñas-Osorio, L. (2014). Multi-dimensional hurricane resilience assessment of electric power systems. *Structural Safety*, 48, 15-24.

Pitilakis, K., Crowley, H., and Kaynia, A. (2014). SYNER-G: Typology definition and fragility functions for physical elements at seismic risk. Dordrecht, Netherlands: Springer, 95-259.

Poulin, C., Kane, M. B. (2021). Infrastructure resilience curves: Performance measures and summary metrics. *Reliability Engineering & System Safety*, 216: 107926.

Qiao, M. M. (2013). Study of evaluation for reconstruction community environment of the towns in Wenchuan earthquake disaster. Master Dissertation of Southwest Jiaotong University. Chengdu, Sichuan, China (In Chinese).

Rose, A. (2007). Economic resilience to natural and man-made disasters: Multidisciplinary origins and contextual dimensions. *Environmental Hazards*, 7(4), 383-398.

Shadabfar, M., Mahsuli, M., Zhang, Y., Xue, Y., Ayyub, B. M., Huang, H., and Medina, R. A. (2022). Resilience-based design of infrastructure: review of models, methodologies, and computational tools. *ASCE-ASME Journal of Risk and Uncertainty in Engineering Systems, Part A: Civil Engineering*, 8(1), 03121004.

Tao, Q., He, Z. (2020a). Measurement of the threshold of community seismic resilience using dynamics-based metrics. *Structural Safety*, 83, 101907.

Tao, Q., He, Z. (2020b). Functionality indicator for an occupant-centred performance model of high-rise residential buildings subjected to earthquakes. *Structure and Infrastructure Engineering*, 16, 1493-1511.

Twigg, J. (2007). Characteristics of a disaster-resilient community: A guidance note. London, U.K.: Department for International Development.

Yin, C., Kassem, M. M., Nazri, M. F. (2022). Comprehensive review of community seismic resilience: concept, frameworks, and case studies. *Advances in Civil Engineering*, 2022, 7668214.

Zhang, W. L., Wang, N. Y., Nicholson, C. (2017). Resilience-based post-disaster recovery strategies for road-bridge networks. *Structure and Infrastructure Engineering*, 13(11), 1404-1413.

NOMENCLATURE

α	Dependence strength coefficient
β	Log-standard deviation of the intensity of ground motions
γ	Topological redundancy
μ	Median of the intensity of ground motions
Ψ	Lognormal cumulative distribution function
ARDP	Accumulative repair durations of preorder entities
BC	Basic component
BD	Building
DS	Damage state
EN	Electricity network
FG	Facility group
PC	Parallel construction
POM	Primary outmigration
PS	Pipeline section
PW	Pathway
RB	Residential building
RC	Repair completion
RD	Repair duration
RP	Repair plan
RS	Repair start
SB	Supporting building
SBF	Collections of functional supporting buildings
SBDF	Collections of dysfunctional supporting buildings
SC	Sequential construction
SN	Sink node
SOM	Secondary outmigration
SR	Source node
ST	Sector
TR	Telecom router
UC	Utility component
UN	Utility network
WP	Water pump
$A_{PWd}(t)$	Adjacency variable of the d^{th} pathway
$C(t)$	Generalized performance function
$G_{RS}(t)$	Repair sequence function
$H_{BC,DS}(t)$	Step function of a basic component in a certain damage state
$i_s(t)$	Normalized post-earthquake staying population of a community
$i_{SOM}(t)$	Population percentage of the secondary outmigration
$I_{POM}(t)$	Population of the primary outmigration
$I_{RB,F}$	Numbers of people living in a fully functional residential building
$I_{RB,O}$	Numbers of people living in an occupiable residential building
$I_{RBg,POM}(t)$	Primary outmigration population of the g^{th} residential building
$I_{RB,S}(t)$	Post-earthquake staying population of a residential building
$I_{RB,T}$	Total population of a residential building
$I_S(t)$	Post-earthquake staying population of a community
I_T	Initial total population of a community
IM_T	Targeted intensity of ground motions
$k(t)$	Normalized toughness of utility networks

$K(t)$	Toughness of utility networks
$K_{UN}(t)$	Probabilistic source-sink connectivity of a utility network
$L_{PSe,P}$	Physical length of the e^{th} pipeline section
$P_{RB,F}(t)$	Probability of the fully functional state of a residential building
$P_{RB,O}(t)$	Probability of the occupiable state of a residential building
$P_{BC,DS}$	Probability that a basic component is in a certain damage state
$P_{BC,O}(t)$	Probability that a basic component is operable (or occupiable)
$P_{BD,DF}(t)$	Probability that a building is dysfunctional
$P_{BD,F}(t)$	Probability that a building is functional
$P_{BD,O}(t)$	Probability that a building is occupiable
$P_{PW,IP}(t)$	Probability that a pathway is impassable
$P_{PW,P}(t)$	Probability that a pathway is passable
$P_{SBh',DF}(t)$	Probability that the h'^{th} supporting building is dysfunctional
$P_{SBh,F}(t)$	Probability that the h^{th} supporting building is functional
$P_{SR\&SN,C}(t)$	Probability that a source node and a sink node is connected
$P_{SR\&SN,DC}(t)$	Probability that a source node and a sink node is disconnected
$P_{UC,O}(t)$	Probability that a utility component is operable
$P_{PSe,F}(t)$	Probability that the e^{th} pipeline section is functioning
$PL_T(t)$	Total probabilistic length of a utility network
$PL_{PSe}(t)$	Probabilistic length of the e^{th} pipeline section
R_E	Resilience threshold
R_L	Cumulative loss
R_T	Recovery period
t	Time variable
$t_{BC,DS,RC}$	Repair completion time of a basic component in a certain damage state
$t_{BC,DS,RD}$	Repair duration of a basic component in a certain damage state
$t_{BC,RD}$	Repair duration of a basic component
$t_{BC,RS}$	Repair start time of a basic component
t_{TRD}	Total recovery duration of a community
$t_{TRD,norm}$	Normalized total recovery duration of a community
$u(t)$	Normalized efficiency of utility networks
$U(t)$	Efficiency of utility networks
$U_{UN}(t)$	Efficiency of a utility network